

Article

A New Look at Physico-Chemical Causes of Changing Climate: Is the Seasonal Variation in Seawater Temperature a Significant Factor in Establishing the Partial Pressure of Carbon Dioxide in the Earth's Atmosphere?

Ivan R. Kennedy ^{1,*}, John W. Runcie ², Shuo Zhang ³ and Raymond J. Ritchie ⁴

¹ School of Life and Environmental Sciences, Sydney Institute of Agriculture, University of Sydney, Sydney, NSW 2006, Australia

² Aquation Pty Ltd., P.O. Box 3146, Woy Woy, NSW 2257, Australia

³ State Key Laboratory of Hydrosience and Engineering, Tsinghua University, Beijing 100084, China

⁴ Faculty of Technology and Environment, Prince of Songkla University, Phuket Campus, Phuket 83120, Thailand

* Correspondence: ivan.kennedy@sydney.edu.au; Tel.: +61-413-071-796

Abstract: Seasonal oscillations in the partial pressure of carbon dioxide ($p\text{CO}_2$) in the Earth's atmosphere, stronger in northern latitudes, are assumed to show that terrestrial photosynthesis exceeds respiration in summer, reducing the $p\text{CO}_2$ in air but increasing its value in winter when respiration exceeds photosynthesis. We disagree, proposing that variation in the temperature of the surface mixing zone of seawater also reversibly regulates the $p\text{CO}_2$ in air as a non-equilibrium process between air and seawater. We predict by thermal modelling that carbonate (CO_3^{2-}) concentration in the surface mixed layer seawater declines in winter by conversion to bicarbonate with CaCO_3 (calcite or aragonite) becoming more soluble and, proportional to the fall of temperature, calcite decalcifying more strongly, allowing more CO_2 emission to air. Paradoxically, the increasing CO_2 concentration in seawater favoring photosynthesis peaking in mid-summer declines simultaneously in autumn and early winter, forced by boundary layer fugacity into phase transfer to the atmosphere, supporting peak atmospheric $p\text{CO}_2$ by late winter. These physico-chemical processes reverse in late winter and spring as seawater warms favoring calcification, fugacity forcing CO_2 from the atmosphere as bicarbonate declines and carbonate increases, augmenting suspended calcite particles by several percent. Our numerical computation predicts that the larger range of thermal fluctuations in the northern hemisphere could reversibly favor absorption from air of more than one mole of CO_2 per square meter in summer with calcite formation potentially augmenting shallow limestone reefs, despite falling pH, if there is a trend for increasing seawater temperature. Another assumption we challenge is that upwelling and advection from deeper water is the sole cause of increases in dissolved inorganic carbon (DIC) and alkalinity in surface waters, even in the southern hemisphere. Instead, some calcite dissolution is favored as water temperature falls near the surface. Standard enthalpy analysis of key DIC reactions indicates why this oscillation is more obvious in the northern hemisphere with seasonal variations in water temperature (ca. 7.1 °C) being almost twice those in the southern hemisphere (ca. 4.7 °C) with a greater depth of the surface mixing zone of seawater in the southern oceans. Questions remain regarding the relative rates of biotic and abiotic inorganic precipitation and dissolution of CaCO_3 in the mixing zone. In summary, rapid biogenic calcification is favored by summer photosynthesis, but slower abiotic calcification is also more likely in warmer water. We conclude that the relative significance of terrestrial biotic and seawater abiotic processes in seawater on the seasonal oscillation in the atmosphere can only be assessed by direct seasonal measurements in seawater.

Keywords: CO_2 ; Keeling curve; Mauna Loa; carbonates; ocean pH; chemical potential; acidification; Henry coefficient; Keeling oscillation; calcite; calcification; ALOHA Station



Citation: Kennedy, I.R.; Runcie, J.W.; Zhang, S.; Ritchie, R.J. A New Look at Physico-Chemical Causes of Changing Climate: Is the Seasonal Variation in Seawater Temperature a Significant Factor in Establishing the Partial Pressure of Carbon Dioxide in the Earth's Atmosphere? *Thermo* **2022**, *2*, 401–434. <https://doi.org/10.3390/thermo2040028>

Academic Editor: Johan Jacquemin

Received: 27 July 2022

Accepted: 8 November 2022

Published: 17 November 2022

Publisher's Note: MDPI stays neutral with regard to jurisdictional claims in published maps and institutional affiliations.



Copyright: © 2022 by the authors. Licensee MDPI, Basel, Switzerland. This article is an open access article distributed under the terms and conditions of the Creative Commons Attribution (CC BY) license (<https://creativecommons.org/licenses/by/4.0/>).

1. Introduction

It is well understood that CO₂ levels in the Earth's atmosphere have increased at about half the rate at which fossil fuels have been combusted globally [1,2]. The conclusion was reached in the Inter-governmental Panel for Climate Change report of 2001 [3] that these observations are directly related, with only half of the CO₂ emissions being reabsorbed by surface biological or physical processes, generating imbalances in the rates of the emission and absorption processes. Particularly for the northern hemisphere, it was assumed by Charles Keeling and colleagues [4,5] that imbalances between photosynthesis and respiratory processes caused surprising oscillations of CO₂ levels ($p\text{CO}_2$) recorded in air of several ppmv above 3000 m on Mauna Loa in Hawaii [5], shown in Figure 1. These seasonal oscillations in $p\text{CO}_2$ extend to the top of the troposphere as observed using spectral occultation from space [6]. By comparison, at Cape Grim, Tasmania in the southern hemisphere only relatively small oscillations are observed, assumed to be a result of less vegetation on land or ocean and limitations on nutrients in seawater. Although smaller than in the Northern hemisphere, seasonal oscillation is nevertheless still present at the Cape Grim site.

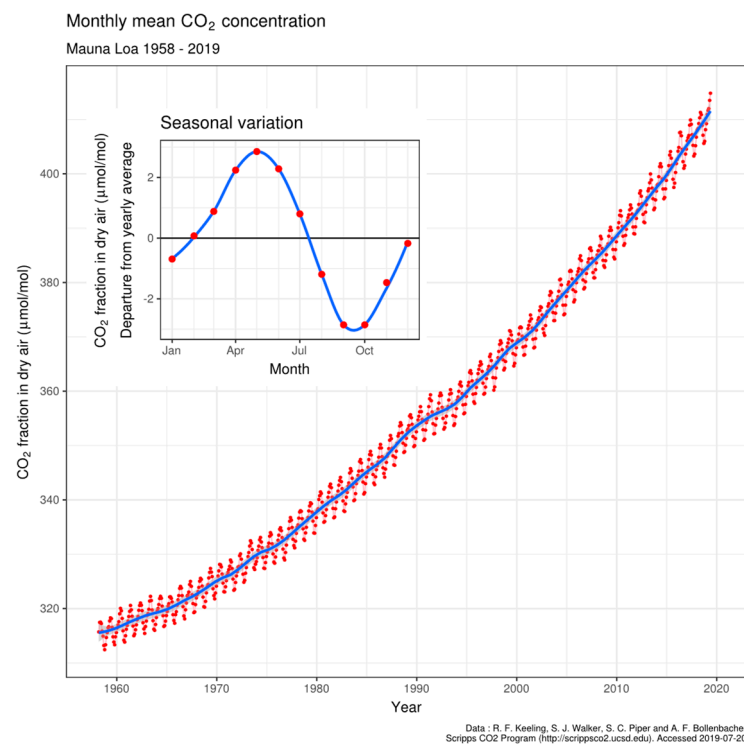


Figure 1. The Keeling curve of atmospheric CO₂ partial pressure at 3200 m on Mauna Loa, Hawaii. Data from Dr. Pieter Tans, NOAA/ESRL and Dr. Ralph Keeling, Scripps Institution of Oceanography. CC BY-SA 4.0, <https://commons.wikimedia.org/w/index.php?curid=40636957>, accessed on 12 November 2022.

Seasonal assessments using observational platforms in the southern latitudes show significant daily variations in carbonate chemistry with some biological activity in sub-polar latitude with more nutrients [7]. Additionally, it has been recognized that the pH of the seawater surface has been falling [8,9], claimed to be a result of the absorption and reaction of CO₂ in surface seawater with carbonate ions, increasing carbonic acid concentration.

It is well established that the seasonal summer decline in atmospheric CO₂ coincides in fertile seawater with higher rates of biotic calcification and acidity, allowing increased CO₂ capture by photosynthesis. However, its reversal in winter is proposed to be also a result of the cyclic dissolution of calcite as temperature falls, facilitated by biogenic respiration now exceeding photosynthesis; this can mutually provide the CO₂ needed to convert carbonate

ion alkalinity from calcite dissolution with bicarbonate increasing. However, other processes may be at work. More recently, it was concluded that variability in ocean circulation and convection in deeper layers is also an important factor in exchange of CO₂ by the ocean [10], explaining some of the variation seen in the annual rise in oceanic CO₂. Here, we will not consider such macroscopic processes, which is important research considered in detail by many studies elsewhere [1,2]. Rather, to help resolve issues of such global complexity, we focus on the mechanistic thermodynamics of interactions occurring at the boundary layers of air and water, in particular testing an alternative thermodynamic cause for the seasonal oscillation observed by Keeling [5]. We advance a testable proposition that seasonal variations in temperature play an important role in establishing rates of abiotic exchange of inorganic carbon between the atmosphere and the surface responsible for the oscillation.

2. Background

2.1. Thermodynamics of CO₂ in Seawater

Given the importance of chemical potentials in this article, some revision is warranted. An important fact regarding CO₂ dissolved in seawater is its small quantity near pH 8 by comparison with the much larger content of bicarbonate (HCO₃⁻) and carbonate (CO₃²⁻); together these carbonic species indicate the total capacity to evolve CO₂ by strong acidification (designated as dissolved inorganic carbon (DIC = [CO₂] + [HCO₃⁻] + [CO₃²⁻])). Another key concept is that of alkalinity due to DIC (A_c = [HCO₃⁻] + 2[CO₃²⁻]) indicating the total equivalents of acid needed for neutralization, releasing CO₂. Insights into thermodynamic concepts such as chemical potential and ideal gas pressure known as fugacity may help clarify environmental behavior of CO₂. At equilibrium, the matching of chemical potentials means that no work is required for a chemical species to move reversibly from one phase to another. However, fluctuations in environmental conditions ensure that conditions of non-equilibrium predominate and spontaneous fluxes of chemical species like CO₂ from one location to another are favored as irreversible processes. These factors (DIC and A_c) impose strong constraints on chemical equilibria, although this may be less rigorous in an open system like seawater because of gaseous diffusion.

The magnitude of the DIC and A_c in global seawater varies with latitude and oceanic basin, largely controlled by temperature, a fact well known since the mid-20th century [10]. For the purposes of our study it is instructive to consider that the current 2022 level of CO₂ of 420 ppmv. corresponds to about 140 moles to the top of the atmosphere above each m² of the Earth's surface. If in reasonably well mixed equilibrium with a seawater surface layer of 65 m depth, a change of 10 μmoles of DIC per kg of seawater would be sufficient to change the pCO₂ in air 1 ppmv. Given that this change in concentration is near the limit of analytical detection in seawater (LOD), we suggest this explains why a relationship with seasonal changes in air has escaped discovery.

Expressing atmospheric gas pressure as parts per million by volume (pCO₂ in ppmv) is not ideal for thermodynamic descriptions involving change in temperature since it is not a measure of concentration. The data in Figure 1 expressed as μatoms per mole are estimated after water vapor has been extracted for gas chromatography. Since humid air can be significantly less dense than dry air since H₂O is lighter than the mix of N₂ and O₂, this practice can overestimate the true concentration of CO₂ in air, unless a suitable correction is made. We can express the average surface pressure of CO₂ in the Earth's atmosphere by the ideal gas law, indicating the number density (N) of molecules per unit volume. In Figure 1, the pressure is given as μatoms of CO₂ per mole of air (i.e., 6.023 × 10²³ molecules), equivalent to ppmv. However, the idea of a heterogeneous mole of air made up of a total of 6.022 × 10²³ different molecules is not useful in thermodynamic terms. The mean partial pressure (p_i) of each gas at the surface per molecule can be given in terms of its number density (N) and the temperature (T).

$$p_i = N_i kT \quad (1)$$

Since the total atmospheric pressure is measured by the gravitational weight of the air per unit area, the balance with thermodynamic factors in Equation (1) containing Boltzmann's constant per molecule (k) the number density (N per unit volume) and the temperature (T) must therefore have an inverse relationship with temperature. This decrease in density with temperature also applies to gas molecules dissolved in water – they will tend to escape as temperature rises, a process captured in the term *fugacity*, meaning fleeing tendency. This property in the gas phase is given as follows, where x_i is the mole fraction ($N_i/\Sigma N_i$) multiplied by the total pressure (p_t), with its correction factor (ϕ).

$$f_{\text{CO}_2} = x_i \phi p_t \quad (2)$$

Like chemical potential, at equilibrium at a given temperature the fugacity must have the same value for all phases, indicating they all support the same vapor pressure, even though the concentrations in each phase will differ, an effect of different chemical environments on chemical potential. In fugacity theory a correction factor (Z -factor) is applied to the concentration in each phase ($C_i/Z_i = f_i$) required to generate the fugacity held in common [11]. For CO_2 in the atmosphere its fugacity (adjusted from Dickson et al. [12]) for a partial pressure of 400×10^{-6} atm (400 ppmv) is 398.743×10^{-6} atm or 40.403 Pa, given 1 atm is 101,325 Pa, with a temperature and pressure sensitive Z -factor of about 0.025 for $[\text{CO}_2]$ at 10^{-5} molal concentration (10 μmolal) in seawater. This difference between fugacity and partial pressure is so small that the departure from ideality (0.3143%) can be neglected in the modelling carried out in this study.

We have the following equalities for concentrations (C) and fugacity of CO_2 .

$$[C_{\text{air}}]/Z_{\text{air}} = f_{\text{CO}_2} \approx p_{\text{CO}_2} \quad (3)$$

$$[C_{\text{sw}}]/Z_{\text{sw}} = f_{\text{CO}_2} \approx p_{\text{CO}_2} \quad (4)$$

The condition of equal fugacity for air and seawater is expressed quantitatively by the Henry's Law coefficient (K_0) that gives the ratio of the molal concentration $[\text{CO}_2]$ in solution to pressure of CO_2 (atm) in the atmosphere, assuming equilibrium between the phases, including temperature.

$$K_0 = [\text{CO}_2]_{\text{aq}}/[p_{\text{CO}_2}]_{\text{atm}} \quad (5)$$

If K_0 increases with decreasing temperature as we will show, a given p_{CO_2} in air will be sustained by a higher $[\text{CO}_2]_{\text{aq}}$ in surface water. Warmer conditions at a given p_{CO_2} in air will reduce the equilibrium concentration needed of $[\text{CO}_2]_{\text{aq}}$ in seawater. A temperature increase in surface seawater need not be considered as causing an increased p_{CO_2} in the atmosphere, unless the DIC concentration in water rises, which is improbable in summer. However, atmospheric p_{CO_2} can increase under colder winter conditions, provided $[\text{CO}_2]_{\text{aq}}$ does also. Establishing this causal relationship is the main topic of this article; this discussion regarding the fugacity of CO_2 is warranted, as will be shown in Section 4.

The Henry coefficient (K_0) is synonymous with an activity factor for CO_2 in the seawater phase; by contrast, the true partition coefficient is given by the ratio of molal concentrations, also equal to the ratio of Z factors in Equation (6).

$$[C_{\text{air}}]/[C_{\text{sw}}] = Z_{\text{air}}/Z_{\text{sw}} = K_{\text{aw}} \quad (6)$$

It is important to understand that the Henry coefficient is not a partition or phase distribution function that indicates a ratio between the amount of substance in each phase (Equation (6)); instead, it is a means to indicate the concentration in water that sustains a certain pressure of a gaseous substance in the atmosphere at equilibrium. This definition has special significance for the processes modelled in this paper. The Henry coefficient can also be expressed [11] as the inverse of Equation (5), but Sander [13] in his comprehensive review

for atmospheric scientists preferred the form given, normal for oceanographers; multiplying the equilibrium $p\text{CO}_2$ by K_0 one obtains the molal concentration of CO_2 dissolved in water that would generate that pressure or fugacity. For convenience in modelling of chemical species expressed as mmoles per kg of seawater, the Henry coefficient is usually given to produce mM concentrations of CO_2 in solution.

2.2. Effects of Temperature on Physical K Values Controlling Steady State Conditions

Regarding daily or seasonal oscillations in the abiotic equilibria for the different species of dissolved inorganic carbon (DIC), CO_2 , bicarbonate and carbonate, shown in Figure 2, changes in temperature must be considered. The Clausius-Clapeyron equation [14] describes the strong effect of temperature on positions of chemical equilibrium, indicating reversible effects on the concentrations of these species with changes in temperature. These fluctuating equilibria are also affected by the reduced $p\text{CO}_2$ in air subject to surface convective forces—or displacement by water vapor that can reach 10% of air volume under extreme conditions. Under warmer air conditions, the lower number density at constant pressure shown by Equation (1) will give a lower chemical potential equilibrating with a lower concentration of CO_2 in seawater. We will demonstrate that the Henry coefficient is reduced at warmer temperature, while K_1 and K_2 governing formation of bicarbonate (HCO_3^-) and carbonate (CO_3^{2-}) increase, discussed following. Importantly for the hypotheses in this paper, the equilibrium shift in dissolved inorganic carbon away from CO_2 and toward increased carbonate is also accentuated by higher temperature, shown conversely by decreasing pK values.

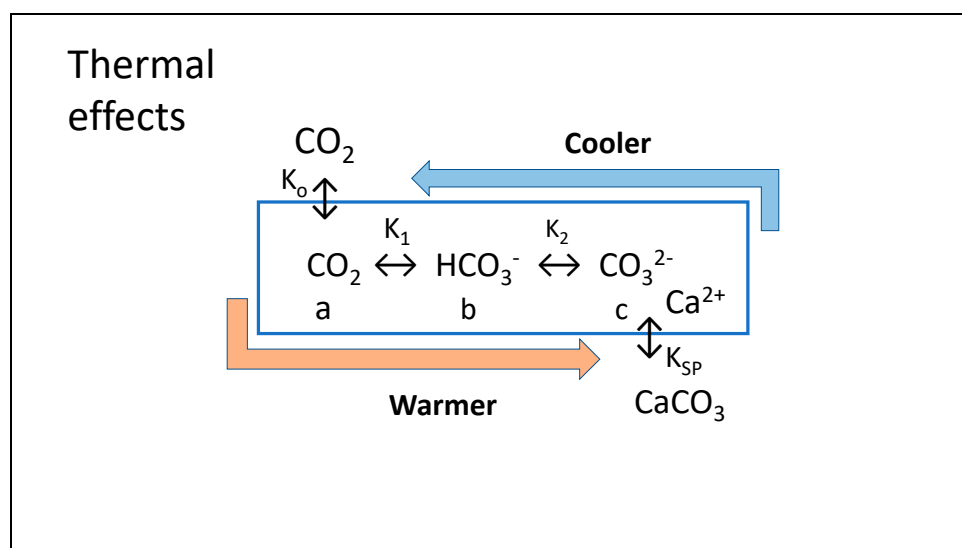
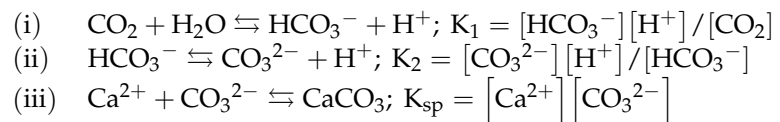


Figure 2. Variations in thermodynamic constants with temperature are proposed to favor precipitation of CaCO_3 in summer with pH falling, coupled with absorption of CO_2 from the atmosphere from spring. In autumn and winter, the process is reversed, dissolving calcite (x moles) and releasing CO_2 to air (y moles), with calcite dissolution in colder water exceeding CO_2 emissions ($x > y$).

This process of carbon transport is further enhanced by a decrease in the solubility product (K_{sp}) with increasing temperature, reducing the amount of soluble carbonate needed in solution for precipitation; the relatively high stable concentration of calcium ions (Ca^{2+} , ca. 400 ppm or 10 mM) in sea water will lead to precipitation of crystalline calcite (CaCO_3) or at least small aggregates as carbonate increases to the point where its ionic product with calcium ions exceeds the current solubility product. For precipitation of calcium ions, it is important to observe that the concentration of calcium ions (Ca^{2+}) in seawater has been estimated by Berner [15] with its activity being only 20% of its molal concentration (ca. 10 mM). In this article, we will assume an activity of 0.20 for Ca^{2+} as estimates to allow ease in recognizing the variation in solubility with temperature.

In our Thermal model shown in Figure 2, it is proposed that as T decreases in winter K_1 , K_2 , c and calcite decrease while K_0 , K_{SP} , a , b increase and $[CO_2]$, $DIC = a + b + c$ and $A_c = b + 2c$ increase, controlled by varying chemical potentials. As T increases in summer, K_1 , K_2 , c , and calcite increase, while K_0 , K_{SP} , a and b decrease as CO_2 , $DIC = a + b + c$ and $A_c = b + 2c$ decrease, but never reaching phase equilibrium. The key reactions that our study models for effects of temperature variation, including K_0 of Equation (5) already discussed above are:



The chemical potentials controlling equilibria for reactions between CO_2 , bicarbonate, carbonate and calcite ($CaCO_3$) will be perturbed by increases in seawater temperature, increasing the equilibrium ratios of HCO_3^-/CO_2 and CO_3^{2-}/HCO_3^- , whilst decreasing the activity of hydroxyl ions, lowering pH. The ionic saturation product for the precipitation of $CaCO_3$ ($[Ca^{2+}] \times [CO_3^{2-}]$) may also exceed the temperature-sensitive solubility product (K_{sp}). It is well established that the solubilities in seawater of anhydrous $CaCO_3$ and $MgCO_3$, counter-intuitively, decline with increasing temperature [16–19]; this property will cause accelerated formation of calcite or aragonite in summer if carbonate ions are near saturation with respect to their solubility product with Ca^{2+} ions. This is particularly the case in the northern oceans where many of Keeling's observations were made. In principle, these feedbacks to increases in temperature could extract CO_2 into water, diminishing its pressure in the atmosphere at all altitudes in summer, explaining the well-known oscillations in pCO_2 noted at Mauna Loa in Hawaii [20]. The magnitude of the oscillation is predicted in this article to be a direct function of the seasonal variation in seawater temperature rather than the kinetic difference between the rates of terrestrial photosynthesis and respiration.

The increasing trend in atmospheric CO_2 since the 19th century is also predicted to be a cause of the increasing acidity of the ocean's surface water [21], with the current anthropogenic emissions of CO_2 mainly responsible. A temperature-based oscillation in atmospheric pCO_2 would require that CO_2 is transported rapidly through the sea surface; this process is subject to rates of boundary layer dispersion as well as longer times for temperature variation—suggested as about a 3-month lag in the oscillation at Mauna Loa. The oscillation is much shorter at Point Barrow in northern Alaska where the surface freezes, holding seawater temperature constant until the thaw in June. The sea's surface pH is a function of the increasing atmospheric CO_2 activity, but also of all inputs of acidity and alkalinity into the ocean.

While warm water contains less dissolved CO_2 , it is obvious that a loss of dissolved inorganic carbon (C) can be accentuated if carbonate ions precipitate with calcium ions (Ca^{2+}), reducing carbonic alkalinity (A_c). Note that thermal precipitation of calcite does not change the absolute alkalinity of seawater, as there is no loss of charge balancing. Yet, the removal of carbonate by reaction with Ca^{2+} ions does remove carbonic alkalinity to an extent that can be titrated if the calcite is removed. In principle, it should be possible to simultaneously withdraw CO_2 from the atmosphere while the solubility product of calcium carbonate is exceeded by the actual product of its ionic concentrations. For data collected from Mauna Loa and elsewhere [3,4] there is a striking seasonal oscillation in the ppmv of CO_2 relative to nitrogen, oxygen and argon. These air samples are dehydrated before gas analysis although daily evaporation of water will also partly control the number density of CO_2 in the atmosphere at the surface, displaced to higher altitude.

Based on these conjectures relying on variations in chemical potential, a testable thermodynamic hypothesis will be proposed. The focus in this article is on abiotic processes, though not to the exclusion of important biogenic processes such as calcification producing protons and soluble CO_2 as described by McConnaughey and Whelan [22].

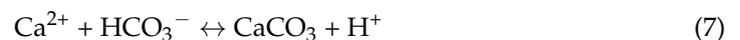
Thermal Hypothesis: *Seawater temperature sufficiently affects chemical equilibria that its seasonal variations cause reversible exchanges between inorganic carbon of atmospheric CO₂ and calcite in seawater (Figure 2).*

This thermal hypothesis is illustrated in Figure 2 for seasonal oscillations in seawater surface temperature. Because of variation in positions of equilibrium at equalized Gibbs potential, DIC alkalinity not only increases in winter as calcite dissolves but the extra alkalinity is more predominantly carried in bicarbonate rather than in carbonate, requiring consumption of dissolved CO₂.

Seasonal assessments using observational platforms in the southern hemisphere show significant daily variations in carbonate chemistry with some biological activity in sub-polar latitude with more nutrients [6–8]. Additionally, it has been recognized that the pH of the seawater surface has been falling, claimed to be a result of the absorption and reaction of CO₂ in surface seawater with carbonate ions, increasing carbonic acid concentration.

However, other processes may be at work. More recently, it was concluded that variability in ocean circulation and convection is also an important factor in exchange of CO₂ by the ocean [9], explaining some of the variation seen in the annual rise in oceanic CO₂. Here, we will not consider such macroscopic processes. Rather, to help resolve issues of such global complexity, we focus on the mechanistic thermodynamics of interactions occurring at the boundary layers of air and land water. We advance a proposition capable of being tested that seasonal variations in temperature play an important role in establishing rates of abiotic exchange of inorganic carbon between the atmosphere and the surface.

Calcification by photosynthetic marine organisms is also favored by this scheme. The following Equation (7) from McConnaughey and Whelan [22] emphasizing proton formation is favored by the variations in Figure 2.



They also explain that the acidifying protons are needed to generate soluble CO₂ needed for photosynthesis.



Although a comprehensive account of calcification is discussed, no mention is made of any role for variation in temperature. The thermodynamic stoichiometry of reactions (7) and (8) may be questioned, although the overall reaction favoring emission of CO₂ is qualitatively correct. Recent data from ZarKogiannis et al. [23] showed that planktonic foraminifera from the central Atlantic Ocean had larger, denser shells in cooler water compared to tropical, possible a result of reduced competition for calcification. However, according to Raven et al. [24] it is unlikely that biogenic calcification has a thermal factor given the rapid diffusion of heat in marine organisms because of their high ratio of surface to volume, unless some special internal metabolic apparatus exists. We will show that higher temperatures favor proton and carbonate formation from bicarbonate by increased K₁ and K₂ values and calcite precipitation as a result of decreased K_{sp}. Thus, in warmer climates, abiotic calcification is predicted to be favored as part of our proposal.

Consistent with this hypothesis, the possible effect of summer warming on precipitating calcite is given in Figure 3, showing increasing values for the Omega supersaturation based on calcium ion concentration as temperature rises, as carbonate alkalinity. Carbonate alkalinity from bicarbonate and carbonate ions decreases with increasing temperature as shown in Figure 3. This is consistent with the increase in Omega (Ω) values for calcite and aragonite shown in the figure, although this fact is mainly a result of the increase DIC as carbonate in summer. Note that Figure 3 plots equilibrium values for the current pCO₂ in the atmosphere as a function of temperature.

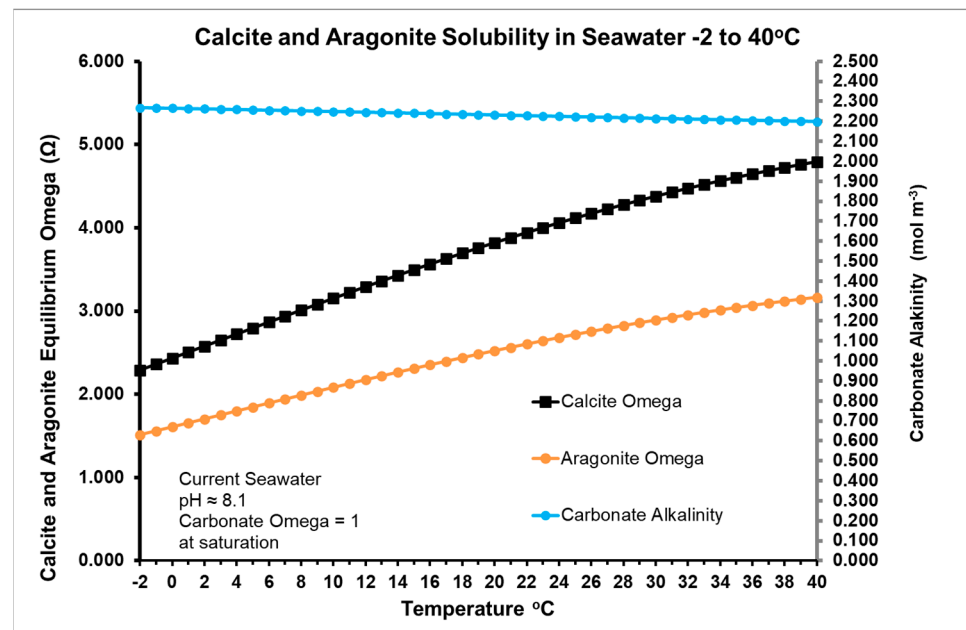


Figure 3. Estimated variation of calcite and aragonite solubility in seawater from -2 – 40 °C for year 2022 CE and Keeling $p\text{CO}_2$ of 421 ppm. Contact RJR if you require a copy of the Excel spreadsheet used for this plot. Omega (Ω) calculations are based on estimates of Ca^{2+} and carbonate activity from the Debye-Hückel theory.

Ω in Figure 3 is the quotient of the ionic product $[\text{Ca}^{2+}][\text{CO}_3^{2-}]$ and solubility product K_{sp} . Since K_{sp} increases with decreasing temperature, more carbonate is needed to precipitate calcite as temperature falls, either with season or latitude.

3. Materials and Methods

3.1. Modelling Strategy and Assumptions

To perform numerical modelling of the control of fluctuating partial pressure of CO_2 by the physico-chemical seawater environment it is essential to define certain general principles. First, these must include a definition for conservation of mass related to seawater. Such a constraint must still have flexible limits, given there are multiple sources for intermediates such as CO_2 . The expression in Figure 2 relating inorganic carbon includes the dissolved forms of CO_2 but it allows fluctuations in atmospheric CO_2 under colder conditions when $[\text{CO}_2]_{\text{sw}}$ as defined by the larger Henry coefficient. So, the conservation of mass is defined within the limits given in the following equation. Note that variations in solid calcium carbonate as crystals has an indeterminate value thermodynamically, with unit activity as anhydrous calcite. For modelling, we usually refer to calcite because the method to estimate solubility is for this anhydrous product, although the more soluble hydrated form of aragonite could also be involved. Calcites less soluble than aragonite, precipitating more readily.

$$C_{\text{T}} = (\text{CO}_2)_{\text{atmosphere}} + [\text{CO}_2]_{\text{sw}} + [\text{HCO}_3^-]_{\text{sw}} + [\text{CO}_3^{2-}]_{\text{sw}} + [\text{CaCO}_3]_{\text{solid}} \quad (9)$$

Second, for the model we designate as Thermal, we need to define the set of fluctuating functions that define positions of the interacting equilibria, given in Figure 2. None of these K values following are constant with temperature variation in the environment, including that for the other significant buffering component in seawater, borate which is included in our model. No other buffering systems usually present in seawater at much lower concentrations such as phosphate or silicates were included in the modelling.

$$K_0 = [\text{CO}_2]/f_{\text{CO}_2} \approx [\text{CO}_2]/[p\text{CO}_2, \text{atm}] \text{ relating the } \text{CO}_2 \text{ dissolved in seawater and air}$$

$$K_{\text{B}} = [\text{B}(\text{OH})_4^-][\text{H}^+]/[\text{B}(\text{OH})_3] \text{ for borate alkalinity}$$

$K_w = [H^+][OH^-]$ for dissociation of water

$K_1 = [H^+][HCO_3^-]/[CO_2]$ for interconversion of CO_2 and bicarbonate

$K_2 = [H^+][CO_3^{2-}]/[HCO_3^-]$ for interconversion of bicarbonate and carbonate

$K_{sp} = [Ca^{2+}][CO_3^{2-}]$ as solubility product of calcite or anhydrous $CaCO_3$

Equations to calculate bicarbonate, carbonate (and even pCO_2) are given in terms of these equilibrium (K) values and hydrogen ion concentrations [12], but these values often are assumed to rely on a constant total value for dissolved CO_2 , bicarbonate and carbonate, suitable for a confined laboratory sample of given volume and composition, but not for an open environment.

Third, the initial conditions for each model must be defined. For the Thermal model, these include variables such as regional seawater temperature, pH in the mixing layer, pCO_2 and others that may be held constant, such as salt concentration (3.50 g/kg) and calcium ions (varying relatively little from 10 mM) or the overall longer term annual trend rate for increasing pCO_2 from various sources. Variables such as $[CO_2]$, $[HCO_3^-]$, $[CO_3^{2-}]$, $[Ca^{2+}] \times [CO_3^{2-}]$ are outputs from the above K functions, responding to changes in temperature, alkalinity, pH and pCO_2 .

The chemical reactions considered in this article are illustrated in Figure 2. The concentrations of dissolved CO_2 , bicarbonate (HCO_3^-) and carbonate (CO_3^{2-}) are calculated as mmoles per kg seawater following oceanographic practice, with CO_2 gas pressure corresponding to ppmv expressed in atmospheres. In tables and graphs, the use of μ moles per kg for output is preferred and ppmv for ease of reading. The chemistry at greater depths is regarded as unchanging in the time scale of the study and is not considered, although it could be relevant. This depth is regarded as representative of the mixed layer although it is recognized as varying from 20–30 m near the equator up to 100–200 m at high latitudes such as near Cape Grim Tasmania where convective and turbulent overturning occurs in much larger parcels of water [1].

Assumptions made in the Thermal model for programming purposes include the following.

- (i) Thermal modelling is not designed to match reality with respect to seasonal dates. Fortnightly periods are used, each period assumed to be separated from the previous by an equal increment in temperature. The primary purpose of the modelling is to estimate effects of temperature variation on carbonate chemistry by season, approximating months and seasons by maxima and minima in temperature or CO_2 concentration. The qualitative results in terms of DIC concentrations or alkalinity are then employed for reasoning regarding causes and effects.
- (ii) Calcite dissolution in winter and precipitation in summer are assumed to be balanced with CO_2 emission to the atmosphere in autumn and winter and absorption in spring and summer. This required an estimate of 65 m depth for the mixing zone in which oscillations of calcite and DIC concentrations occur. Each meter depth (cubic meter) is assumed to contain about 1000 (near 1025) kg of seawater per square meter of surface, so approximately 1000 times molal values are given for each meter of depth, or some 65 times this amount for the entire surface mixed layer.
- (iii) Equal increments of calcite dissolution and precipitation are given numerically as fortnightly jumps, with adjustments to K values recalculated separately for changes in temperature and then atmospheric pCO_2 . The procedure makes inputs of carbonic alkalinity from calcite dissolution and then solves a quadratic equation for bicarbonate concentration, relating this to carbonate and CO_2 concentration based on the new equilibrium constants with the incremental change in temperature. The quadratic equation is generated by equalities for carbonate concentration based on bicarbonate (Equation (10)).
- (iv) While the Thermal hypothesis is focussed on inorganic chemistry, it is not assumed that biogenic calcification and calcite dissolution is completely independent, or that processes of advection and convection in seawater do not contribute to these processes. Such processes may be essential in contributing to the scale of the abiotic processes proposed in Figure 2. Deciding the relative contributions to seasonal calcification

and calcite dissolution may require future research given that we aim to show how physical effects of seasonal temperature variation may be needed to fully explain the relationship between the boundary layers of the ocean and the atmosphere.

3.2. Software

Full details of the model program coding called Thermal generated for this study are given in the Supplementary Materials. This program calculates variation in equilibrium constants with temperature and chlorinity according to the algorithms of Emerson and Hedges of 2008 [2]. The algebraic logic of the programmable Texas Instruments SR52 was chosen for modelling purposes, because of its simplicity and ease of use. The precision of calculation in the SR52 program was to 21 significant figures so all modelling results are correct to the accuracy of the input data, given that the number of incremental iterations never exceed 13 with no rounding errors. Rewriting this code given in Supplementary Materials in higher level languages such as R, Mathematica, Python or Java is suggested for those interested in repeating this study, particularly for easier graphical illustration. There are at least 10 computing packages available for calculating key inorganic properties of DIC in seawater [25] based on the principle of setting input pairs of variables to particular values and then calculating all other values of interest.

The relevant literature cited in this article is highly valued by us for its role in forming hypotheses and by supplying suitable algorithms for calculating changes with temperature in thermodynamic constants for seawater. The specific algorithms used in our program of Emerson and Hedges [2] depend on the work of many preceding authors that were also consulted, including Wells [15], Saruhashi [26], Pales [4], Gieskes [27], Pytkowicz [28], Mehrbach et al. [29], Ingle [30], Plath et al. [12], Mucci [16], Dickson and Millero [31], DoE [32], Millero [33], Millero et al. [34], Bailey et al. [35] and Watson et al. [36]. For example, the equation of Mucci [17] based on earlier research [12,18,29,30] was employed to establish the temperature dependence of the stoichiometric solubility constants of calcite. The values estimated for K_{sp} near 4.2×10^{-7} for calcite employed in the Thermal model, are two orders of magnitude larger than those given in textbooks for fresh water. The clear ideas expressed in these papers have made this article possible.

To simplify numerical computation, the concentrations of intermediates were routinely abbreviated as is customary: $[CO_2]$ as a , [bicarbonate] b and [carbonate] as c . A flow sheet for the Thermal model is shown in Figure 4. Periodic variations in values (mM) for carbonic alkalinity (A_c) and total inorganic carbon (C_T) were provided by reiteration in coding, allowing for changes in temperature or in emission reducing C , or absorption of CO_2 or variation in calcite content (varying A_c). Changes in factors such as pCO_2 , concentration of CO_2 , bicarbonate and carbonate can be programmed with versatility. For example, being able to calculate equilibrium constants with variations in temperature [31] enables $[CO_2]$ and pCO_2 to be estimated from inputs of alkalinity, pK and pH values alone. Alternatively, pCO_2 and temperature changes can be used to generate values for alkalinity (A_c) and dissolved inorganic carbon (DIC) compounds (C). Given likely time delays in equilibration for atmospheric pCO_2 values with seawater $[CO_2]$, the Henry coefficient was adjusted to 0.85 times its equilibrium value to allow the product of $[Ca^{2+}]$ and $[CO_3^{2-}]$ to exceed 1.0 for comparisons during cooling or warming processes. This suggests that that input values for fCO_2 using reported pCO_2 values for air are excessive, perhaps not properly corrected for environmental factors such as humidity, yielding DIC values higher than observations.

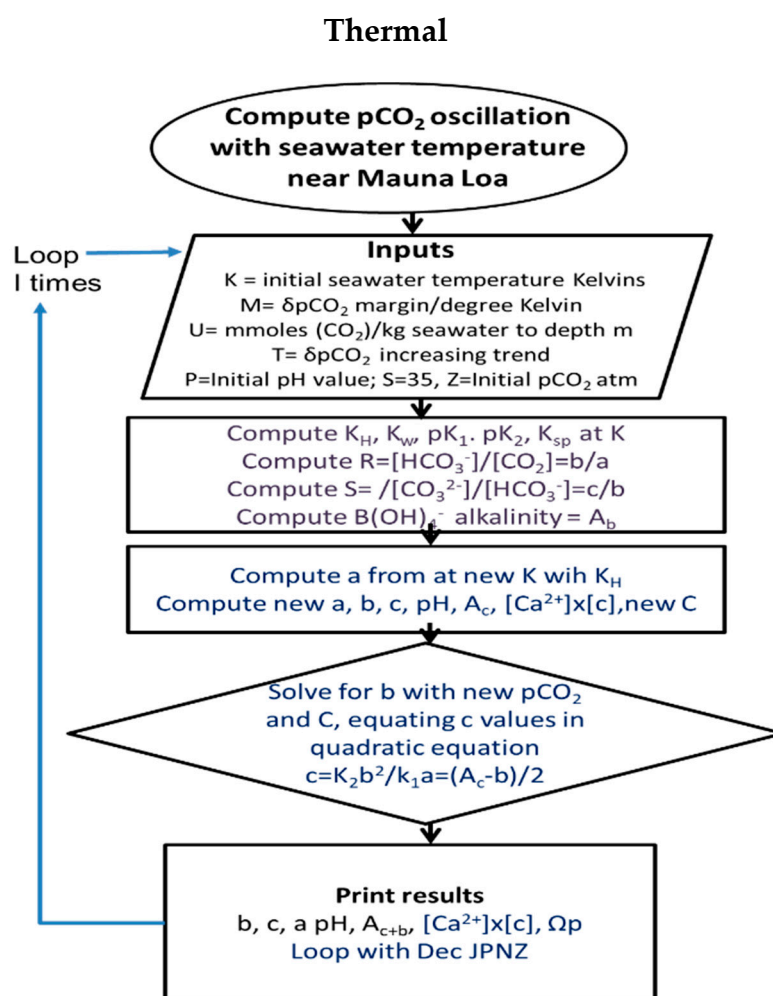


Figure 4. Flow diagrams for Thermal programs, generating changes in $p\text{CO}_2$ in response to changes in temperature. A copy of the code is provided as Supplementary Material or directly from the corresponding author.

Although the variations in equilibrium constants with temperature are regarded as accurate, environmental systems rarely reach equilibrium. While equilibrium is likely in the short term for carbonic reactants dissolved in surface layer seawater, it is difficult to predict the extent of disequilibrium where inorganic carbon passes from one phase to another at the water surface or in formation or dissolution of anhydrous calcite. In the Thermal model, where CO_2 passes from seawater to air, any disequilibrium can be simulated numerically by adjusting the value of the Henry coefficient downwards so that the concentration in solution is slightly reduced for a chosen atmospheric $p\text{CO}_2$. This could be a result of a lag time for equilibration from air to seawater. Alternatively, the $p\text{CO}_2$ may not have been corrected for dilution by thermodynamic pressure from surface water vapor. If surface air is saturated at $25\text{ }^\circ\text{C}$, it will have a mixing ratio for water of 0.0216 kg per kg . Water being 1.61 times lighter than dry air molecules, the surface atmospheric pressure is supported thermodynamically by 3.48% of water vapor, reducing the CO_2 concentration estimated from fugacity at 420 ppmv in dry air to 410.35 in saturated air.

3.3. Solving Thermal Carbonic Concentrations

In Figure 4, a program flow sheet is shown. Inputs of current inorganic carbonates contents, carbonate alkalinity and pH values are required. Each program iteration of the seasonal temperature change ($\delta T/26$) commencing in late summer at the minimum value of

atmospheric $p\text{CO}_2$ inputs adds a moiety of carbonate alkalinity, resetting all K equilibrium values for 26 periods and solving for concentrations of CO_2 , bicarbonate and carbonate.

A key element in the programming was the use of a standard quadratic equation solution to find approximate values of bicarbonate concentration (b) as input variations in $p\text{CO}_2$ and $[\text{CO}_2]$ or alkalinity (A_c) occurred. This solution is based on the equalities that $K_2/K_1 = ac/b^2$ and $A_c = b + 2c$, thus solving by equating carbonate ion (c) in these two relations as follows; we then solve for bicarbonate (b) with estimates for current new inputs of CO_2 (a) or alkalinity (A_c).

$$\text{Carbonate} = c = (K_2/K_1a)b^2 = (A_c - b)/2.$$

Then

$$(2K_2/K_1a)b^2 + b - A_c = 0 \quad (10)$$

This allows bicarbonate (b) to be obtained from the quadratic solution $x = \{-b \pm (b_q^2 - 4ac)^{1/2}\}/2a$, taking care not to confuse the quadratic factor b_q (+1) in Equation (10) with the b for bicarbonate in the solution; the term x in the quadratic is equal to $[\text{HCO}_3^-] = b$, thus solving the equation.

Each reiteration recalculated all constants and DIC species at the new temperature allowing direct computation of $a = [\text{CO}_2]$ from the Henry coefficient, estimating b and c using the new K_1 and K_2 values and then pH, total DIC (C) and alkalinity (A_c and A_t) before estimating CO_2 vented to the atmosphere with an equivalent transfer of calcite, recalculating a and the new value of bicarbonate (b) using a quadratic equation with the new alkalinity value A_c . This operation was regarded as occurring in an open system, with calcite dissolving and CO_2 being transferred within the water column more freely.

4. Results

4.1. Thermodynamics and Van't Hoff Estimation of Enthalpy

An analysis of the variation in key constants involved in modelling (Figure 4) defining their values with changes in temperature are shown in Table 1. The Henry coefficient varies most strongly with temperature favoring a lower gas concentration in seawater $[\text{CO}_2]_{\text{sw}}$ compared to the equilibrium air pressure $p\text{CO}_2$ (atm) as temperature rises. Thus, the fugacity of CO_2 in solution increases with temperature. Note the wide range of values between 278 and 298 K for the Henry coefficient (K_0) in seawater proportional to temperature as predicted by the ideal gas equation, estimated using Equation (4) for number density as moles per liter. The molarity in air only decreases from 18.4 μmolar to 17.2 μmolar over the same decrease in temperature, maintain a gas pressure of 0.00042 atm. The decreasing pK_1 and pK_2 values with increasing temperature means that the respective K_1 and K_2 values increase with temperature, increasing the equilibrium ratios of bicarbonate to CO_2 and of carbonate to bicarbonate, thus favoring precipitation of calcite. A smaller effect is caused by the decrease in solubility constant (K_{sp}) for calcite with increasing temperature.

Thermodynamic behavior trending to increase carbonate ion activity $[\text{CO}_3^{2-}]$ in summer and bicarbonate activity $[\text{HCO}_3^-]$ in seawater in winter is central to the main hypothesis given in this article. The variation in the dissociation of water (K_w) is also significant, contributing to the large variation in K_0 indicating CO_2 solubility. True neutrality in seawater at pH 7.0 appears to occur only near 280 K, reducing to pH 6.6 at 298 K, coinciding with a maximum value for K_{sp} as water changes its structure. Clusters of water molecules are larger in colder water, with reduced ionization shown by the ten-fold reduction in dissociation constant; this means that hydrogen ion activity measured as pH 7 or the pH 8.2 of seawater is associated with a higher activity of hydroxyl ions in warmer water. The values generated using the program for K_0 , K_1 , K_2 and K_w at 25 °C, with a salt concentration chlorinity index of 35‰ and 1 atm pressure are almost identical with those in the comparison made by Orr et al. [24] of the ten packages available that compute ocean carbonate chemistry.

Table 1. (a) Estimated variation with temperature of equilibrium constants used for modelling of surface seawater at $p\text{CO}_2$ air 420 ppmv; (b) Standard enthalpy, Gibbs energy and entropy changes for the K_1 and K_2 equilibria.

(a)									
Temperature K	°C	$K_0 = Z_{\text{sw}}$	pK_1	pK_2	$K_w \times 10^{14}$	pK_w	$K_{\text{sp}} \times 10^{-7}$ [Ca ²⁺][CO ₃ ²⁻]	μmolar CO ₂ in seawater	
278.15	5	0.05213	6.042	9.292	0.855	14.07	4.309	21.90	
283.15	10	0.04388	5.984	9.203	1.443	13.84	4.317	18.43	
288.15	15	0.03746	5.931	9.118	2.380	13.62	4.315	15.73	
293.15	20	0.03241	5.882	9.035	3.839	13.42	4.300	13.61	
298.15	25	0.02839	5.837	8.955	6.063	13.22	4.272	11.92	
Results varying with temperature estimated with software in Supplementary Materials (Item 4)									
(b)									
Temperature K	°C	pK_1	ΔH° kJ/mol	ΔG° kJ/mol	ΔS° kJ/K	pK_2	ΔH° kJ/mol	ΔG° kJ/mol	ΔS° kJ/K/mol
278.15	5	6.042	17.490	32.301	−0.053	9.292	26.837	49.672	−0.081
283.15	10	5.984				9.203			
288.15	15	5.931	16.273	32.698	−0.057	9.118	26.751	50.152	−0.081
293.15	20	5.882				9.035			
298.15	25	5.837	15.059	33.160	−0.061	8.955	26.771	50.900	−0.082

Estimates made with pK results from (a) using software in Supplementary Materials (Item 5) for Equation (11).

Supporting a role for thermodynamics in seawater, standard values per mole for enthalpy change for the two main DIC equilibria in Figure 2 using the van't Hoff relation [14] shown in Equation (11) are given in Table 1(b), estimated for pairs of temperature in the range 278.15 – 298.15 K; also given are changes in standard molar Gibbs energy ($\Delta G^\circ = -RT \ln K_{\text{eq}}$) and entropy ($\Delta S^\circ = (\Delta H^\circ - \Delta G^\circ)/T$).

$$\ln(K_{T_2}/K_{T_1}) = -\Delta H^\circ(1/T_2 - 1/T_1) \quad (11)$$

The thermodynamic values obtained are similar over this 20 K temperature range, given that the Van't Hoff equation is acknowledged to be approximate, even for minor changes in temperature. The strongly positive endothermic values estimated for enthalpy of both reactions given in Table 1 are consistent with heat being absorbed by the system and with the decrease in entropy. A positive value for standard enthalpy is qualitatively consistent with warmer water favoring more formation of bicarbonate from CO₂ and carbonate from bicarbonate in summer, a process reversed in winter when heat is released as carbonate is converted to bicarbonate and bicarbonate to CO₂. We regard this result as strong thermodynamic information consistent with the Thermal hypothesis.

4.2. Modelling the Thermal Hypothesis

A preliminary model run (see Supplementary Material for programming details) tested how the $p\text{CO}_2$ pressures generated in the atmosphere might vary with monthly seawater temperature at Hilo, Hawaii (Big Island). However, the result in Table 2 of just over 1 ppm $p\text{CO}_2$ variation of in this temperature range of 2.2 K is too small to support a hypothesis that variations of 7 ppmv are possible. This possibility may have been considered previously by researchers in this area, then dismissed. Further, the model was run with constant pH—unnatural for the environment. Thus, some other variable factors need to be included before a thermodynamic explanation for the Keeling oscillation can be obtained. However, the observation in Table 2 that the relative ratio (Ω) of the saturation product for calcite

($[\text{Ca}^{2+}] \times [\text{CO}_3^{2-}]$) over the solubility product (K_{sp}) exceeded 1.0 (shown bolded) at the warmest temperatures was a useful finding, helping to justify proceeding with this Thermal hypothesis. An early estimate for Ca^{2+} ion activity in seawater near 0.2 [15] has been assumed in this model analysis, but an exact value is not required since only the relative seasonal variation with temperature is needed.

Table 2. Results of numerical modelling (Jan–Dec) showing DIC concentrations for intermediates between CO_2 and calcite varying with changes in regional seawater temperature at constant pH.

		Jan	Feb	Mar	Apr	May	Jun	Jul	Aug	Sep	Oct	Nov	Dec
a	CO_2	10.70	10.75	10.81	10.70	10.60	10.48	10.40	10.27	10.19	10.27	10.38	10.59
B	HCO_3^-	1740.	1742	1745	1740	1735	1730	1727	1720	1716	1720	1726	1735
C	CO_3^{2-}	214.8	213.9	212.7	214.8	217.3	219.8	221.7	224.9	226.5	224.9	222.0	217.3
C	Sum	1766	1967	1968	1966	1963	1961	1959	1955	1954	1955	1958	1963
Ab	Borate	2262	2261	2261	2262	2262	2263	2264	2265	2265	2265	2264	2262
K _{sp}	$\times 10^{-7}$	4.27	4.27	4.28	4.27	4.27	4.27	4.27	4.27	4.26	4.26	4.27	4.27
$[\text{Ca}^{2+}]$	$\times [\text{CO}_3^{2-}]$	4.25	4.24	4.21	4.25	4.30	4.35	4.39	4.45	4.49	4.45	4.49	4.3
Ω	Ratio	0.995	0.991	0.985	0.995	1.007	1.020	1.029	1.045	1.052	1.045	1.030	1.007
pH		8.05	8.05	8.05	8.05	8.05	8.05	8.05	8.05	8.05	8.05	8.05	8.05
K	Temp..	298.	297.8	297.6	298.0	298.4	298.8	299.1	299.6	299.8	299.6	299.1	298.4
$p\text{CO}_2$	ppmv	375.1	375.2	375.3	375.1	374.9	374.7	374.5	374.2	374.0	374.2	374.5	374.9
Ac	Alkalinity	2170	2170	2170	2170	2170	2170	2170	2170	2170	2170	2170	2170

Run with program titrate allowing $p\text{CO}_2$ values to be calculated from pH, pK and alkalinity (Ac) values. Results shown are modelled for seawater temperatures at Hilo, Hawaii from a minimum of 297.60 in March to a maximum of 299.80 in September. Ab is Ac alkalinity including the borate system.

This hypothesis makes the novel proposition that changes in the temperature of seawater simultaneously affect chemical equilibria so that seasonal variations (Figure 1) can cause reversible exchanges between inorganic carbon in atmospheric CO_2 and calcite in seawater, with a flux of inorganic carbon from seawater to the atmosphere in winter and its reabsorption forming calcite in summer. The hypothesis is tested in the knowledge that other factors including biota may also affect the CO_2 pressure and the formation or dissolution of calcite. A primary test of the hypothesis can be conducted in a computer model to examine covariation of these thermodynamic factors, successfully performed here. Other tests can be conducted in the laboratory, or the field using tools such as ^{14}C -labelled calcite to test variation in solvation discussed later. Table 2 shows variations in temperature and concentrations of intermediates suggesting precipitation of calcite for the relative ratio Ω greater than 1.0, as occurs in steps 5–12. No change in alkalinity was programmed, which is only possible if no acids are absorbed, giving constant pH value. Only slight changes in the solubility product occurs with change in temperature, slightly lower in summer when carbonate concentration reaches its maximum, facilitating calcite formation in this season

Thermal model: This numerical Thermal model outlined in Figure 4 first recalculates the effect of fluctuations in temperature on all equilibrium constants for the reactions of Figure 2—the Henry’s coefficient (K_0) for $p\text{CO}_2$, constants for reversible formation of bicarbonate (K_1) and carbonate (K_2) as well as the solubility product (K_{sp}) for calcite (CaCO_3). The intensity of the trend with temperature will be related to the rates of processes such as decreases in chemical potential or increases in entropy of CO_2 with temperature [10], as well as the rate of decreased solubility of calcite [27,34].

Table 2 is indicative of the operation of this Thermal variation model, a trial being run with constant alkalinity and pH value, varying temperature but lacking processes of calcite formation or dissolution. Small changes are shown for redistribution between DIC species, a decline in carbonate in March when bicarbonate and CO_2 are maximal. Variations in

$[\text{CO}_3^{2-}]$ and K_{sp} for calcite are sufficient to nominally precipitate calcite shown by the Ω factor exceeding 1.0, using an activity for $[\text{Ca}^{2+}]$ of 0.20 to highlight its greater likelihood.

However, there is no reason that pH and alkalinity in an open system need be constrained and the Thermal program was revised to allow pH variation, calculated from pK values and bicarbonate or carbonate ratios. It was more important to determine the effect on DIC and carbonic alkalinity, dissolving calcite in a winter process of low temperature and transferring DIC to the atmosphere.

4.3. Oscillation of $p\text{CO}_2$ on Mauna Loa

The model output in Figure 5 and Table 3 using the revised coding allowing alkalinity and pH variation shows how the intermediate equilibria are predicted to shift in seawater during cooling from the warmest seawater temperature of 299.8 K (26.65 °C) in September to 297.6 K (24.45 °C) in March, as measured nearby in Hilo, Hawaii. As a result of shifts in the equilibria with temperature varying 2.2 °C, carbonate is predicted to decrease 6.2 $\mu\text{moles per kg}$ seawater, with bicarbonate and CO_2 increasing by 71 and 0.77 $\mu\text{moles per kg}$, respectively during cooling from September to April, dissolving calcite. The flux of CO_2 to the atmosphere from dissolving 2.5615 $\mu\text{moles calcite per kg}$ for each of 13 cooling temperature periods is predicted to be 2.1645 moles per square meter, emitted from some 65 tonnes of well-mixed seawater; this could occur more intensively from a lower volume nearer the surface. Calcite solubility increases as shown by the decline in the ratio for relative saturation (Ω) from 1.019 to 0.987 as seawater cools.

For simplicity, the model assumes that the variations of temperature and $p\text{CO}_2$ are periodic, but the results given are not designed as functions varying with time but as functions of change in temperature. The intention was to illustrate the effect of temperature variation on the scale of thermodynamic properties. However, the range of $p\text{CO}_2$ values and seawater temperatures do match those typically observed in the region, with the model calibrated to give a change of $p\text{CO}_2$ in air of 7 ppmv at Mauna Loa for each half-year; this included a longer-term superimposed upward trend of 1.8 ppmv per annum as shown in the Keeling curve (Figure 1).

These predictions may need adjustment to local conditions and the oscillation in $p\text{CO}_2$ may be associated with a larger seasonal temperature range given the CO_2 mixing ratio in the atmosphere is derived from a larger area around Mauna Loa, Hawaii. For example, using the same program with a 5 K range between 292 and 297 K assuming the same dissolution rate for calcite to be emitted as CO_2 , bicarbonate and $[\text{CO}_2]$ increased by 107.8 and 1.6 $\mu\text{moles per kg}$ of seawater with carbonate decreasing from 296.3 to 261.3 $\mu\text{moles per kg}$, about six times greater than the range of 2.2 K at Hilo, with a larger increase in pH value. This demonstrates the sensitivity to temperature, including the effect of lower winter and summer temperatures. Earlier research [35] on the effect of variation of temperature on the pressure of CO_2 , perhaps perversely, claimed that warmer seawater from Woods Hole released more CO_2 . However, that experiment used a closed system and observation was clearly a short-term result consistent with operation of the Henry's coefficient, reducing the amount of dissolved CO_2 . In the field over a longer time span, the model predicts the now obvious alternative that CO_2 can flow reversibly en masse through an open system, becoming first carbonate and then mainly calcite, as seawater warms in a system near calcite saturation.

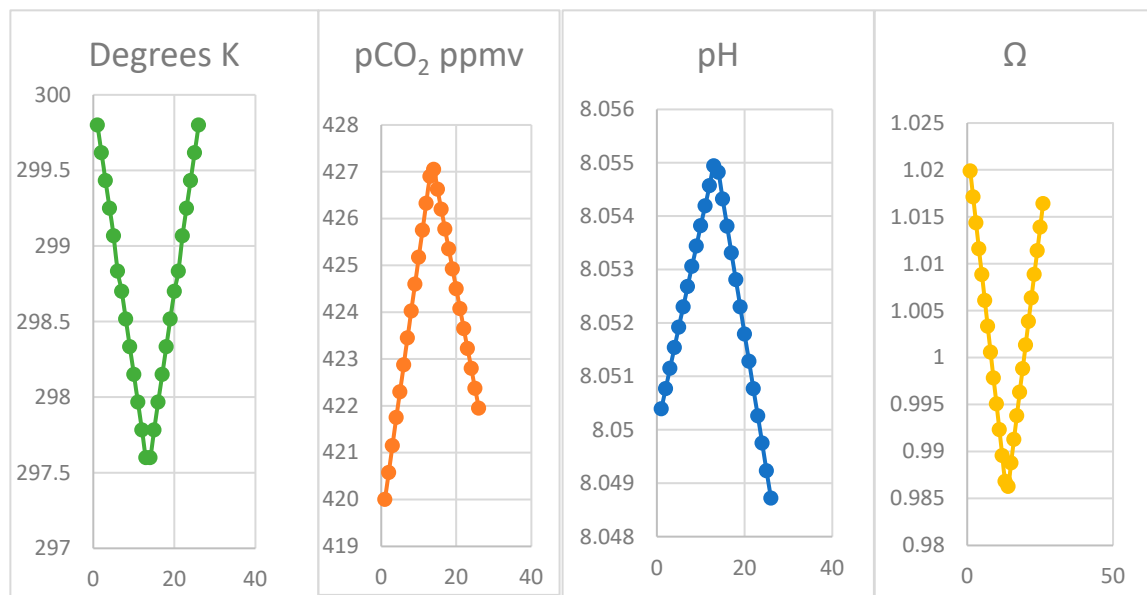


Figure 5. Estimated variations (Oct–Sep) in seawater temperature, pH and saturation (Ω) for calcite at Hilo and $p\text{CO}_2$ on Mauna Loa for 26 periods per year (x -axis, temperature \times time); only for temperature is the original condition regained.

Table 3. Results from Thermal program of cooling process from peak seawater temperature to minimum (I = 12, M = 0.0000005, DIC U = 0.0025615, P = 8.05, S = 35).

Month	Oct	Nov	Dec	Jan	Feb	Mar	Apr
δT	1	2	3	4	5	6	7
a CO_2	9.84	9.90	9.96	10.02	10.08	10.14	10.20
b HCO_3^-	1658	1664	1669	1675	1680	1686	1691
c CO_3^{2-}	218.8	218.2	217.7	217.2	216.7	216.2	215.6
DIC	1887	1892	1897	1902	1907	1912	1917
Ac	2096	2107	2104	2109	2113	2118	2122
Ab	2191	2195	2199	2203	2207	2212	2216
Ω	1.017	1.014	1.011	1.008	1.006	1.003	1.000
K	299.8	299.6	299.4	299.3	299.1	298.8	298.7
$p\text{CO}_2$	420.0	420.6	421.2	421.8	422.3	422.9	423.5
pH	8.050	8.051	8.051	8.052	8.052	8.052	8.053

See Supplementary Materials for full 12-month dataset; I = No. iterations, M = $p\text{CO}_2$ margin, U = mmoles calcite.

A major role for marine biota in achieving observed rates of these thermal adjustments in DIC is not excluded, provided sufficient growth nutrients exist. For example, precipitation of calcium carbonate by phytoplankton during photosynthesis either internally or externally is a normal function of their metabolism [22]. The model in Figure 2 proposes that the DIC equilibria shift towards carbonate and proton formation favouring calcification in summer, generating the higher CO_2 activity needed for photosynthesis while increasing the rate of calcification, including that of the more soluble aragonite compared to calcite.

Our modelling outputs shown in Figure 5 and partly in Table 3 follow the observations for $p\text{CO}_2$ at 3200 m altitude on Mauna Loa very closely. The model assumes the actual monthly seawater regional temperatures measured at Hilo, generating the corresponding range of $p\text{CO}_2$ observations. It predicts corresponding values for alkalinity (A_c), total dissolved inorganic carbon (C) and individual activities of CO_2 (a), bicarbonate (b), carbon-

ate (c), the pH value as well as the saturation of calcite (Figure 5). The close quantitative correspondence of the $p\text{CO}_2$ and the temperature pattern and the feasibility of the inorganic process, even for such a narrow temperature range, suggests that the assumption of the oscillation being caused exclusively by imbalances between photosynthesis and respiration, mainly on land, could be rejected. Particularly in a maritime region where rates of processes vary little from temperature changes, biological processes on land for cycling carbon may be near balance, at the warm low latitudes of the Hawaiian Islands.

The x-axis in Figure 5 indicates model data outputs for 26 iterations in temperature for 4.4 K of reversible temperature variation in 12 months, shown in Table 3 for six months from October to April from autumn to spring. As shown in Table 3, increases in CO_2 , bicarbonate, DIC and alkalinity (A_c and A_b) occur, with carbonate decreasing while adjustments to alkalinity from calcite dissolution while temperature declines. Only inorganic responses to changes in temperature are shown, generating only a small increase in dissolved CO_2 . In the absence of biotic reactions, only a small increase in pH value occurs, despite the increase in CO_2 . However, the increase predicted in bicarbonate and DIC is substantial, explaining increase in pH value. In Figure 5, note that all factors other than temperature are asymmetrical caused by the ongoing trend in $p\text{CO}_2$ value; solubility of calcite increases 0.3% annually unless temperature increases. The primary data shown in Figure 5 unsurprisingly all give linear responses, since they are equal differentials in temperature. The actual time course of temperature for seawater at Hilo could be modelled, possibly giving a closer correspondence with time in field data, but with no material advantage. The testing of the physical hypothesis in the model shows it is consistent with the proposal. Experimental confirmation by actual laboratory and field studies under appropriate conditions is strongly recommended.

We conclude from this simulation that the DIC in the ocean surface layer could tend to equilibrate with the CO_2 level of the atmosphere, responding to changes in surface temperature. This should be confirmed by satisfactory laboratory and by examining the many marine field studies, to be discussed in Section 4. Greater variations in temperature more typical of middle latitudes in the Pacific ocean would magnify the variations shown in Figure 5.

The data shown in Figure 5 are given as a complete dataset in Supplementary Materials, for a 12-month period of 26 two-week periods commencing in October at the maximum water temperature. The scale is not time, but the segmented temperature. Two sets of outputs for each temperature are shown, one for the effect of variation in temperature and a second for that generated following addition of a slug of CO_2 . Full details of the program is given as listed in Supplementary Materials available on-line. Note that during the onset of winter concentrations of both bicarbonate and CO_2 increase together with carbonic alkalinity (A_c) and DIC while carbonate (c) decreases, proportional to the temperature difference. In the subsequent summer season, all these results are reversed.

Although temperatures taken at Hilo, Hawaii were employed in the model, in fact the variation in $p\text{CO}_2$ in Hawaii obviously would be influenced by the seawater temperature covering a much larger area of seawater.

4.4. Larger Oscillations at Point Barrow, Alaska

The oscillation in $p\text{CO}_2$ measured by Keeling and colleagues on the northern coast of Alaska at Point Barrow is even more striking in its magnitude than at Mauna Loa (Table 3). The seawater temperature is almost constant for seven months of the year controlled by the effects of ice in brine (Figure 6). The $p\text{CO}_2$ stays constant on a plateau during the winter period, only falling in late summer from July to December as seawater warms a total of 4.4 °C. This pattern is claimed to represent stronger photosynthesis on the tundra in summer but it is also easily explained as a thermodynamic response to seawater temperature. The precise correspondence between temperature and changes in $p\text{CO}_2$ is striking, corresponding to the plateau effect. The variation in seawater temperature is twice

that observed at Hilo nearest Mauna Loa, explaining the characteristic steeper gradient of $p\text{CO}_2$ in the summer months and a doubling of its magnitude.

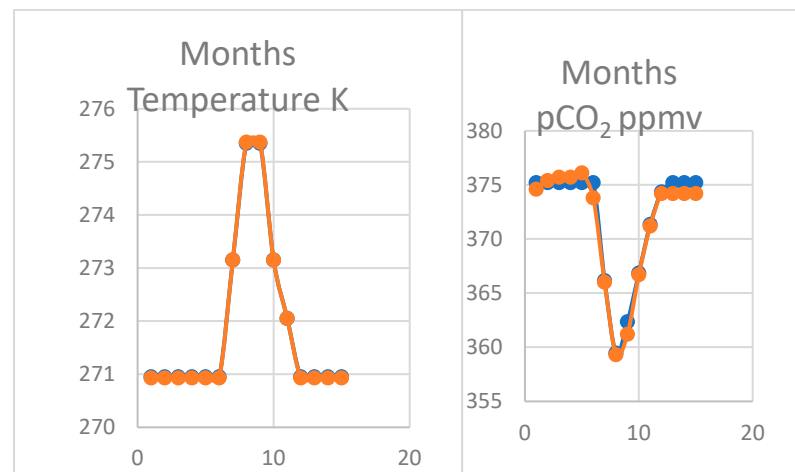


Figure 6. Estimated variation in $p\text{CO}_2$ (right) with temperature (left) January to December at Point Barrow, Alaska showing a plateau in winter months falling in summer, consistent with modelled reduced solubility shown in Supplementary Materials. Thus, CaCO_3 is predicted to be dissolved when seawater is colder from November to June.

The Thermal program was employed to model the effects of changes in temperature (Figure 7). As for Mauna Loa, results were output twice at each stage shown in Supplementary Materials, once for each change in temperature and again when alkalinity was reduced from formation of calcite in warming water with atmospheric CO_2 declining or the in reverse when temperature to cooling. The primary data also show that the ratio of the corrected ionic product and the solubility product or the saturation constant (Ω) only exceeds 1.0 in the three summer months, suggesting that CaCO_3 is augmenting at the same time as the $p\text{CO}_2$ is falling. The result shown in Figure 6 is consistent with the longer-term trend for 1974–2009 [4] at Point Barrow.

Using temperature data from Point Barrow as shown in Supplementary Materials, the model was run at a higher pH value of 8.26 consistent with Arctic conditions [37], automatically generating a higher alkalinity under the much lower temperatures at Barrow. This is predicted to occur at the lower seawater temperature at Point Barrow near freezing. It is not certain, however, that calcite is the proper crystalline form of calcium carbonate formed under frigid conditions [37,38], where crystalline ikaite [38] may be formed; this is a hydrated form of crystalline CaCO_3 with a K_{sp} ten times less (ca. 6×10^{-8}), showing it could be more easily precipitated with less alkalinity. Ikaite is regarded as too soluble to precipitate at warmer temperatures [38]. Takahashi and Olafsson [39] showed that at the onset of summer there is a rapid onset of photosynthesis at the thaw consuming nutrients of nitrate and phosphate rapidly but the consumption of CO_2 they observed of 100 μmoles per kg corresponding to Redfield values for nutrients only accounts for about half the diminution in $p\text{CO}_2$ in air per square meter that continues to decline after the nutrients are exhausted, rising again as seawater freezes.

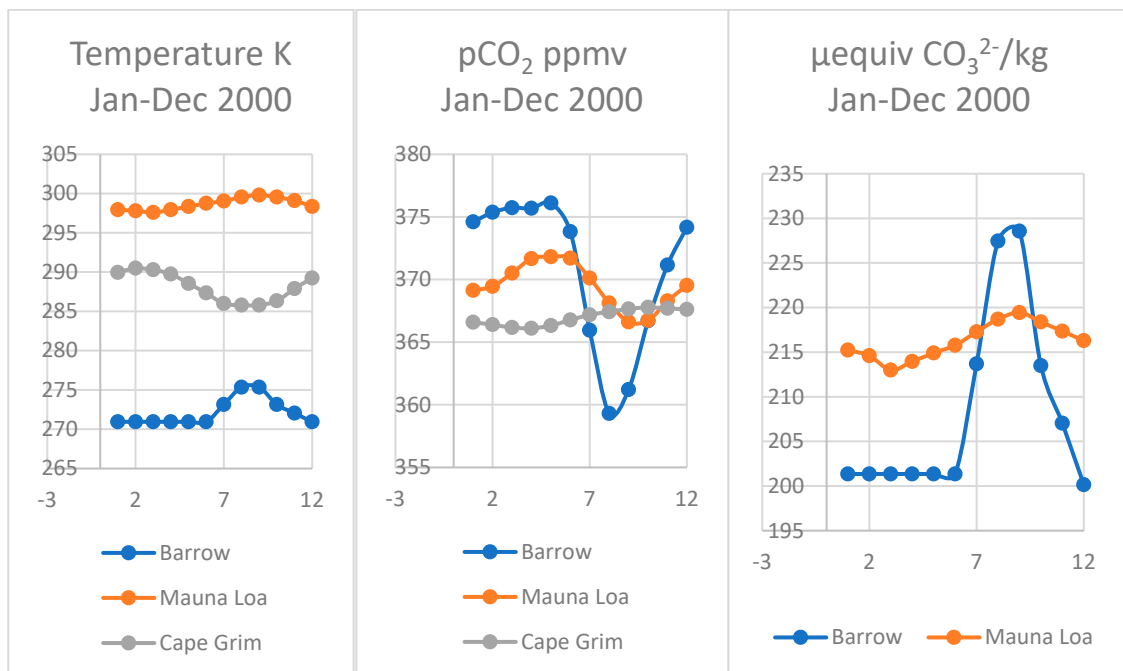


Figure 7. Comparison of actual data recorded for surface seawater temperature and $f\text{CO}_2$ and estimated carbonate using the Thermal model for seawater at Point Barrow Alaska, Mauna Loa Hawaii, (Keeling et al., 2009) and near Cape Grim (CSIRO) at Smithton, Tasmania.

4.5. Comparing Cape Grim, Tasmania and Sites at Mauna Loa and Point Barrow

Although similar seasonal oscillations in $p\text{CO}_2$ for greenhouse gases have been observed in the southern hemisphere at Cape Grim on the north-western corner of Tasmania [1], these are much lower than the annual trend curve for increasing CO_2 , in contrast to those in the northern hemisphere, particularly in the Pacific basin. The mean seawater temperature near Cape Grim is lower at 14.8°C than at Hilo, Hawaii where it is 28.4°C , but higher than at Point Barrow near freezing (Figure 7).

5. Discussion

In 2003, Zeebe and Westbroek [40] defined a simple model for the CaCO_3 saturation states of the ocean as three alternatives (“Strangelove, Neritan and Cretan”), the latter demonstrated by actual inorganic precipitation in surface seawater shown as ‘whittings’, either as by biogenic shallow water precipitation with settling under gravity or with low precipitation, remaining effectively in solution. However, there was no discussion of seawater temperature and its effect on these states. In this article, we draw attention to what might be considered a fourth active state preserving mass but defined as promoted by warmer surface temperature. The extent of augmentation of calcite in summer or dissolution at a maximum would be little more than 1% of the DIC, near the limit of analytical sensitivity. Yet, this could be sufficient to explain the scale of seasonal oscillation in the atmosphere of some 2 moles of CO_2 moles per m^2 of the Earth’s surface.

5.1. Deciphering the Station ALOHA Data Sets as Establishing Non-Equilibrium between Air and Seawater

Estimates of $p\text{CO}_2$ or equilibrium with dissolved $[\text{CO}_2]$ either directly by equilibrated gas phase infra-red measurements [41] or by calculation using formulae can show major variations in values where biological activity and organic breakdown is likely, as in coastal sampling. The Station ALOHA dataset (see Supplementary Materials) show peaks in estimated $[\text{CO}_2]$ in seawater in late summer, with maximum acidity (minimum pH values) at the same time as the atmospheric oscillation $p\text{CO}_2$ is minimal, clearly not equilibrated. Peak $p\text{CO}_2$ in air occurs in late winter, although there is a preceding small pause in mid-

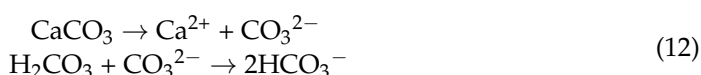
winter. In our Thermal model, inputs of carbonate from dissolution of calcite resulted in equivalent increases in DIC and in alkalinity (A_c) in winter. Such a CO_2 in surface seawater could indicate nutrient depletion with respiration exceeding photosynthesis in autumn.

However, Quay and Stutsman [42] explained this as a result of ingress of CO_2 from the atmosphere, or from upwelling. This enables the ALOHA dataset in the 1990s to be accommodated by the biogenic assumption for the oscillation but Karl Popper suggests this is poor science compared to obtaining data capable of falsifying the hypothesis. At the same time, the DIC is minimal, having declined about 12–20 $\mu\text{moles per kg}$ seawater from a peak in April. They claimed variation in carbonic alkalinity was negligible although their plot of this data could readily be interpreted as similar to the change in DIC. The maximum temperature in this surface water in October coincided with the greatest decline in DIC. In addition, the fact that the mixing zone reached almost twice the depth in winter, could mean that the seasonal variations in DIC and alkalinity could be about 30 $\mu\text{moles per kg}$, not dissimilar.

More recently, Chen et al. [43] have simultaneously quantified atmospheric $p\text{CO}_2$ versus surface seawater $f\text{CO}_2$ for samples taken within a meter of the boundary since 2002 in the North Pacific region, also using a novel satellite-based $p\text{CO}_2$ seawater model with inputs of ocean color at the Woods Hole Hawaii Ocean Time-series (WHOT) in the North Pacific gyre at ALOHA Station. They claim evidence for large scale forcing from a natural Pacific Decadal Oscillation imposed on increases near 2 $\mu\text{atom yr}^{-1}$ for the Keeling increase, with the atmospheric rate exceeding the seawater rate of increase in $p\text{CO}_2$ by 0.5 $\mu\text{atom yr}^{-1}$. The same pattern for comparisons between air and seawater $f\text{CO}_2$ values apply as seen in the ALOHA Station, with peak values almost opposite in phase between summer and winter.

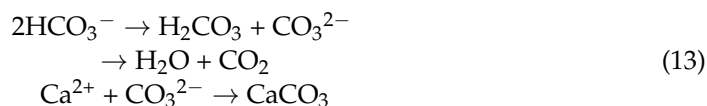
What can explain this apparently paradoxical result, showing that equilibration in fugacity between the air and seawater is never achieved, but with the latter greater for a significant period of several months after mid-summer, before the minimum pressure in air? Thus seawater fugacity decreases simultaneously with air fugacity increasing the maximum value in late winter. Chen et al. [43] do not discuss the period of several months when $p\text{CO}_{2\text{sw}}$ exceeds $p\text{CO}_{2\text{air}}$ (shown in Supplementary Materials) regarding their recent data from the WHOT Station, focused on showing how the increasing value in the former forces that latter perhaps in agreement with the terrestrial assumption with respect to the source of the seasonal oscillation in air. In our model results from October at Mauna Loa shown in Figure 5, the input of dissolved carbonate in winter to fully match the change in $p\text{CO}_2$ of the atmosphere takes into account a surface layer of around 65 m involving some 65,000 kg of seawater. Each iterative increase in $p\text{CO}_2$ in air of 0.5 ppmv would require 2.5615 $\mu\text{moles CO}_3^{2-}$ dissolution from calcite, assuming that each ppmv in air is equivalent to 0.333 moles of CO_2 in the total of 140 moles per m^2 for a $p\text{CO}_2$ of 420 ppmv. However, this requirement reflecting the $[\text{CO}_2]$ activity usually expressed as potential $f\text{CO}_2$ in seawater reaches a maximum in midsummer when the modelled atmospheric $p\text{CO}_2$ value approaches its least value.

However, a logical explanation for the discrepancy between phases is available if the minimum values in seawater of $[\text{CO}_2]$ or $f\text{CO}_2$ later in midwinter may reflect consumption of CO_2 as H_2CO_3 reacting with carbonate from dissolving calcite at the lower temperature, shown in Equation (12).



This process was not included in our Thermal model applying to Table 3 and Figures 5–8 although it could be to provide a more authentic process. The purpose there was to show how the equilibrium compositions for DIC would need to move to equilibrate with changes in temperature and alkalinity. It is consistent with the highest pH values in the ALOHA dataset on removal of CO_2 as carbonic acid to dissolve calcite. A general correlation is that each change of 10 ppm in $p\text{CO}_2$ in air corresponds to a pH change of 0.01 units, although the biotic variations in these factors are like much greater than those predicted for abiotic

reactions (Figures 5 and 6). Just as the biotic process of photosynthesis increases in spring and early summer, there would be a rapid decrease in seawater pH value as CO₂ is released as carbonic acid from the bicarbonate pool and calcite clusters augment with sufficient warming. This process (Equation (13)) is thermodynamically favored as the equilibrium shifts from bicarbonate to carbonate ions as seawater warms.



This biological pH shift will contribute to increased carbonate ion activity in summer and in the solubility index (Ω), as is predicted for abiotic processes in summer (Table 3). It may be difficult to quantitatively separate the thermodynamic effects of the two calcification processes, biotic and abiotic, with both contributing to a depletion of atmospheric CO₂ in summer as calcite or aragonite is precipitated. It is noteworthy that the $p\text{CO}_2$ on Mauna Loa falls slightly just before midwinter as CO₂ is consumed to convert carbonate to bicarbonate, as is required in the Thermal model and Equation (12). It is proposed also that CO₂ within the surface seawater layers could be sufficiently mobile by diffusion between the mixing zone and slightly deeper water. Given a difference in chemical potential caused by the variation in surface temperature its diffusion will be accelerated. A variation in the chemical potential of [CO₂] for 5 K difference (Table 1) could cause a significant flow of dissolved CO₂ sufficient to overcome this difference. Given that chemical potential is a logarithmic function of concentration, this temperature difference would require a doubling of the CO₂ concentration. Alternatively, as mentioned previously, in winter respiration fueled by organic carbon fixed in the previous summer can provide the CO₂ required.

Table 4 illustrates thermodynamic properties that vary by phase, seawater or air. The processes of transfer of CO₂ to air and of calcite dissolution are both shown to be endothermic. The small standard Gibbs energy change for CO₂ transfer indicates a reverse in relative ease of thermodynamic transfer between 288–298 K temperature. These values favor transfer of CO₂ to air in mid-summer and the reverse in winter as the flow to seawater occurs, shown in Figure 8. The fugacity Z factors for air or water are very different with change in temperature, about seven times as responsive in seawater, reflecting structural changes of the aqueous medium such as reduced clustering. The concentrations of CO₂ in seawater shown in Table 4 for each temperature can be calculated as equal at 18 μM at 280 K, the temperature where calcite reaches maximum solubility. As discussed in Section 2.1, this means that the chemical potential for CO₂ in seawater is much more responsive to changes in temperature than its chemical potential in air. Given the fact that the mixing zone for the ALOHA Station data was stated by Quay and Stutsman [42] as twice as large in winter than in the summer doldrums, the total quantity of CO₂ estimated for the mixing zone in winter must be greater than that produced in the mixing zone in summer. Furthermore, while CO₂ in surface air is slightly denser in winter, its chemical potential is significantly less affected by change in temperature in air than in seawater, the Z-factor varying only 0.0007 in air versus 0.0040 in surface seawater for a temperature change of 5 °C. Comparing the variation of physico-chemical activity of CO₂ in air with that in seawater using a fugacity or pressure measurement (μatoms for ppmv) as given in Figure 1 must be carefully done at each temperature.

Table 4. (a) Modelled estimates of thermodynamic variation of key constants with temperature of seawater and its concentration using the Thermal model; (b) Standard enthalpy, Gibbs energy and entropy changes for the K_{aw} and K_{sp} equilibria.

(a)								
K	Temperature °C	$K_0 = Z_{sw}$	Z_{air}	$K_{aw} =$ Z_{air}/Z_{sw}	$K_{sp} \times 10^{-7}$ [Ca ²⁺][CO ₃ ²⁻]	μ_{CO_2} $\times 10^{-27}$ J	μM CO ₂ in dry air	
278.15	5	0.05213	0.04324	0.8295	4.309	−9.1660	18.16	
283.15	10	0.04388	0.04248	0.9681	4.317	−9.3482	17.84	
288.15	15	0.03746	0.04174	1.1143	4.315	−9.5307	17.53	
293.15	20	0.03241	0.04103	1.2660	4.300	−9.7135	17.23	
298.15	25	0.02839	0.04034	1.4029	4.272	−9.8966	16.94	

Z_{air} shows inverse variation in temperature, at 420 ppmv; Z_{sw} includes variation in solubility of CO₂ in seawater; software in Supplementary Materials (Item 4).

(b)										
K	Temperature °C	K_{aw}	ΔH° kJ/mol	ΔG° kJ/mol	ΔS° kJ/K	K_{sp} $\times 10^{-7}$	ΔH° kJ/mol	ΔG° kJ/mol	ΔS° kJ/K/mol	
278.15	5	0.8295	20.234	0.249	0.071	4.309	+2.241	34.198	−0.121	
283.15	10	0.9681				4.317				
288.15	15	1.1143	18.950	−0.263	0.064	4.315	+0.302	35.125	−0.123	
293.15	20	1.2660				4.300				
298.15	25	1.4029	14.923	−0.709	0.059	4.272	−0.970	36.042	−0.125	

Software to compute standard energy changes included in Supplementary Materials (Item 4).

Even though the diminution of surface DIC in summer in ALOHA Station data from 1994 to 1999 can be modelled in terms of rates of absorption CO₂ from air or dynamic seawater mixing, it is also consistent with effects of temperature on positions of equilibrium as proposed in Figure 1. The fact that there is no close correspondence between seawater and air in CO₂ analyses emphasizes how far from formal equilibrium these processes in seawater and air are and the magnitude of time lags for transfer; such lags mean that while air is gaining CO₂ in autumn and winter while calcite is dissolving, seawater is losing it; while air is losing CO₂ in summer as calcite precipitates, seawater is gaining it. Furthermore, basing transfer rates from one phase to the other purely on this comparison under non-equilibrium conditions may be partly mistaken. For example, the values calculated or estimated from seawater samples represent averages and other factors such as short-term oscillations between day and night where seawater may be warmer than air at the surface may affect the direction of transfer. Could the dynamic sea surface represent a Knudsen barrier [44] where a tendency to concentrate molecules in the cooler phase according to the square root of respective temperature apply? Specific research is needed.

However, the results of Chen et al. [43] allow CO₂ transfer from the peak value of pCO_{2sw} in mid-summer to its minimum value in mid-winter as shown in Figure 8. Their data collected at the ALOHA WHOT Station involved simultaneous measurements of pCO_{2air} and of pCO_{2sw} using infrared analysis of samples collected just above and just under the surface showing the lack of equilibrium between the air and seawater phases at the boundary layer. They focused on the forcing of the process of CO₂ transfer from air to seawater giving an increasing trend because of terrestrial emissions of CO₂. However, for several months the pCO_2 supported by seawater samples from early summer exceeds that in air favoring, transfer proportional to the difference.

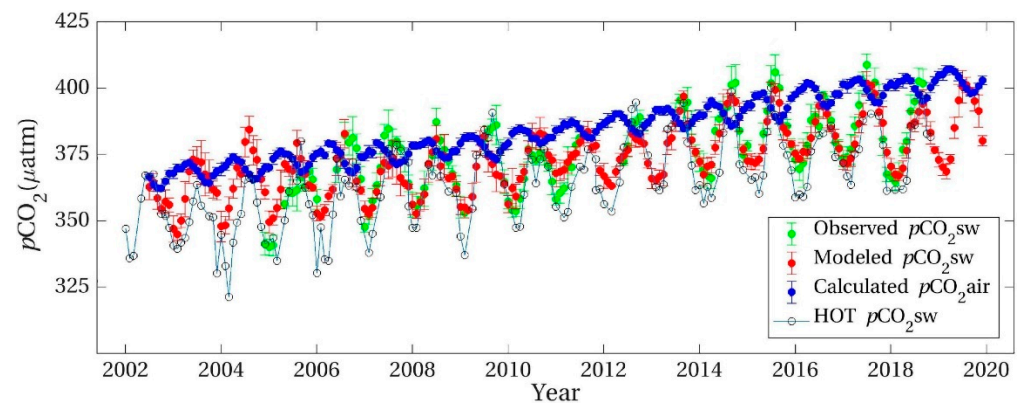


Figure 8. Seasonal WHOT non-equilibrium oscillations in simultaneous $p\text{CO}_2$ measurements in seawater and air [43,45] (y -axis divisions $5 \mu\text{atm}$) showing converse values suggesting transfer of CO_2 to air in autumn and, more strongly from air to seawater in spring. Peak and minimum seawater surface temperatures were 1–2 months after mid-summer and mid-winter with ranges of about 4 K, twice that modelled for Hawaii in Figure 5 and Table 3.

We intend in future to apply fugacity analysis according to Mackay [11] for diffusion between phases. This could be applied to datasets like those in Figure 8, taking into account the exactly inverse nature of the Henry law constant (H) and the Henry coefficient (K_0) employed in this article. While concentration (corrected if necessary for activity) is a satisfactory driving force for diffusion within a phase it is unsatisfactory as a force for diffusion between phases. At equilibrium between the phases, a chemical's fugacity on both sides of the interface will be equal. The differing Z factors in each phase shown in Table 4 correct concentrations in each phase for fugacity. It can be assumed that a solute like CO_2 will be transferred rapidly in the mixing zone of seawater by eddy diffusion of parcels of water, minimizing the concentration and temperature gradient. However, near the interface the eddies are damped and a mass transfer coefficient with physical dimensions of velocity operates, in part a function of concentration difference between the phases. It is assumed [11] that the following relationship holds.

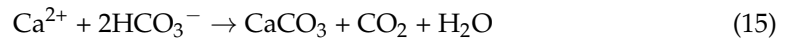
$$[\text{CO}_2]_{\text{air}}/[\text{CO}_2]_{\text{sw}} = K_{\text{aw}} = Z_{\text{air}}/Z_{\text{sw}} = = 1/K_0RT \quad (14)$$

Given that in mid-summer and autumn, the solubility of CO_2 in seawater is minimal (Table 4) and its content in air is also minimal, transfer from seawater to air is facilitated, in terms of the fugacity force causing transport [11], N (moles/hr) = $D_V (f\text{CO}_{2\text{sw}} - f\text{CO}_{2\text{air}})$, where D_V , a composite of mass transfer coefficients, is the total conductance for transport between the two phases. In mid-winter to spring when these fugacity terms are reversed with $f\text{CO}_{2\text{air}}$ at its maximum and $f\text{CO}_{2\text{sw}}$ minimal.

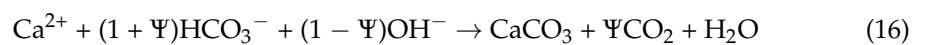
The fact that the chemical potential of bicarbonate is predicted in the Thermal model to be substantially less negative in autumn to winter as bicarbonate concentrates at the expense of carbonate thus has an important role in the rate of replenishment of seawater CO_2 ; this can be compared to the situation in mid-summer of highest $p\text{CO}_2$ in seawater favoring photosynthesis while bicarbonate is predicted to be depleted as thermodynamics favors its conversion to carbonate and calcite, also releasing carbonic acid according to Reaction (12). Some published data for $p\text{CO}_2$ values in air may not have been corrected downwards for dilution of CO_2 by water vapor, possibly in error more than 5 ppmv as a function of humidity. However, Chen et al. [43] carefully distinguished between $x\text{CO}_2$ mole fraction values and $p\text{CO}_2$ in air, the former for dry air as in Table 4 and the latter always corrected for dilution by saturated water vapor, based on methods developed by Sutton et al. [45].

5.2. Interpreting Stoichiometry of Reaction between Bicarbonate and Calcium Ions

Smith [46] and others have questioned the stoichiometry of the qualitative calcification [22] reaction (13). For example, Chen-Tung and Pytkowicz [47] pointed to the acidifying effect from oxidation of biogenic detritus as consuming alkalinity, resulting from oxidation of reduced nitrogen and sulfur moieties to strong acids. Such a process could also contribute to reduced alkalinity in winter when respiration is predominant.



In effect, Equation (13) links photosynthesis to the formation of CaCO_3 so that the carbonic acid resulting can yield carbohydrate plus oxygen. However, an extensive analysis of field data by Smith [46] based on research data collected by others suggested that the following equation with different stoichiometry was more appropriate near the surface, producing less CO_2 for each calcite molecule formed.



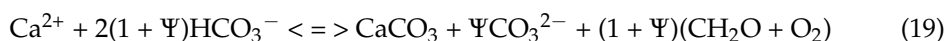
The static or steady state Ψ factor favored was found to be near 0.6 for surface seawater, although it is nearer 1.0 as in Equation (16) at greater depth, a requirement if overall seawater DIC and the atmospheric CO_2 are to be naturally balanced [46]. If 100 μmol per kg of calcite was precipitated from water with known values of DIC and alkalinity A_c and then normalized by return to the water's starting $f\text{CO}_2$; this precipitation in Equation (15) qualitatively reduces carbonate alkalinity by 200 μmoles per kg and the $f\text{CO}_2$ of the water at a given temperature rises, then degasses to reach the previous value. That is, the system is concluded to be constrained by equilibrium with $p\text{CO}_2$. However, the Ψ factor is by no means a constant as Smith shows but varies to some extent with environmental conditions such as seawater depth as well as the presence of other buffering systems or strong acid, such as borates or phosphates or organic anions. The latter are the main source of alkalinity in plants. Smith did not offer a source for the alkalinity of ca. 0.4OH^- ions per molecule of CaCO_3 formed. Incidentally, perhaps Equation (16) would have been written more logically subtracting $(1 - \Psi)\text{H}^+$ ions from the left side instead, producing less water but still maintaining charge and mass balance and the same amount of CO_2 . In effect, $(1 + \Psi)$ bicarbonate ions would be converted to $(1 + \Psi)$ carbonate ions and 2Ψ protons, producing CaCO_3 and Ψ carbonic acid molecules, shown in Equation (17).



A similar analysis but considering the effect of the seasonal variation in temperature, DIC and carbonic alkalinity, factors not considered by Smith [45], would differ in stoichiometry. In summer precipitation of CaCO_3 as shown in Equation (18) would be caused by warming, proposed in Figure 2. In winter, a reverse process increasing carbonic alkalinity (A_c) induces an increase in bicarbonate with decrease in carbonate as in the Thermal model. This decrease in carbonate in colder water as K_2 decreases can be equated to Ψ in Equation (16), but sufficient CO_2 must also react to convert all the dissolved carbonate from calcite plus the diminishing carbonate previously in the seawater pool to bicarbonate as shown in Table 3 for the Thermal model. This CO_2 can be sourced from carryover from winter to summer, or biotically from ongoing decomposition, or even by rapid diffusion from lower in the seawater profile, responding to a thermodynamic deficit. Overall, in winter this could consume $(2 + \Psi)$ molecules of CO_2 to gradually vent one molecule to the atmosphere, supported by the conversion of the two sources of carbonate to bicarbonate, equilibrating towards increased $[\text{CO}_2]$ in winter in seawater. It is possible that the value of Ψ may differ for forward and reverse directions, dependent on factors like temperature.

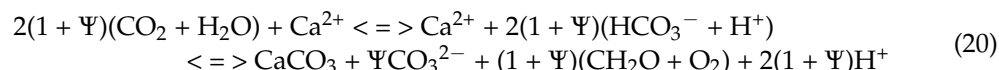


As shown, also increasing carbonate in summer as predicted in the Thermal model (Table 3), the seasonal mixing zone reaction (Equation (18)) to the right indicates the summer process releasing CO₂ as CaCO₃ is precipitated. Fortuitously, this provides the CO₂ needed from its major source in seawater of bicarbonate for the coupling of calcification to biogenic processes [22] involving increased photosynthesis producing carbohydrate (abbreviated CH₂O) in summer (Equation (19)).



While the formation of carbonate and calcite is thermodynamically favored in summer temperatures, as predicted in the Thermal model, biosynthetic processes require the absorption of sufficient photons contained in sunlight.

Paradoxically, the reverse reaction consuming CO₂ to increase bicarbonate in winter, that we propose also raises the tendency to achieve equilibrium [CO₂] concentration in seawater and thus the increase in *p*CO₂ in the atmosphere, can result from a mutualistic or even symbiotic process between biotic and abiotic reactions. The moiety of CO₂ required in winter to absorb the alkalinity (*A_c*) by converting carbonate to bicarbonate is proposed to be from biogenic oxidation of organic carbon or detritus in the oxic zone near the surface or from anaerobic respiration with inorganic sulfate as the most prevalent oxidant in deeper seawater. This process of generation of carbonic acid naturally reduces the pH value of seawater but its consumption in converting carbonate to bicarbonate restores the pH value as more alkaline. As written above, Equation (19) is incomplete to agree with the Thermal model, lacking the following addition shown in Equation (20), including charge balancing protons.



We recommend that rather than Equation (15), this equation be used as the formula of choice for calcification and its relationship between productivity as photosynthate and atmospheric CO₂. Note that charge balance requires that the formation of calcite from Ca²⁺ ions produces the net two H⁺ ions formed in Equation (20) and that conversion of bicarbonate to carbonate requires formation of carbonic acid. It is assumed that the elevated bicarbonate concentration in winter predicted in the Thermal model will ensure transfer of CO₂ to the atmosphere, equivalent to the dissolution of calcite aided by CO₂ from oxygenic respiration of photosynthates formed in summer. Possibly, in nutrient-deficient seawater the CO₂ required in winter could be augmented by diffusion of CO₂ through the interface at the base of the mixing zone, driven thermodynamically.

The magnitude of (1 + Ψ) in the Thermal model was found proportional to the variation in temperature. If no variation in temperature is considered as in the data examined by Smith [45], the ratio of bicarbonate to carbonate is less affected and consequently less CO₂ is required to allow for a change in alkalinity. If such a mutual relationship between bioorganic and inorganic processes is responsible for much of the seasonal oscillation it is not surprising that this proposal has been slow to emerge to clear understanding. These seasonal reactions in winter and summer involve consumption and release of CO₂ in seawater could also be responsible for the larger seasonal excursions in seawater pH values in the ALOHA WHOT datasets [43]. Although the summer reaction with decreasing *A_c* alkalinity generates decreased pH values, this will be accentuated by the significant release of CO₂ as the haze of calcite augments. In winter the increased pH value observed in the modelling from October to May will also be greater as a result of the consumption of CO₂ generated biogenically.

This conclusion is consistent with ‘snapshot’ ALOHA Station data that show a maximum in [CO₂] concentration and lowest pH value in seawater in summer, favoring photosynthesis followed by a minimum in [CO₂] and maximum pH in winter (see Supplementary Materials); this suggests the consumption of CO₂ in the reverse reaction with carbonate by Equation (19) and significant escape to the atmosphere with a thermodynamic potential

for $[\text{CO}_2]$ supporting a higher atmospheric $p\text{CO}_2$. As mentioned earlier, peak levels of $f\text{CO}_2$ estimated in seawater [43] occur in mid-summer about three months before $p\text{CO}_2$ in air reaches a minimum in October before starting to rise as $f\text{CO}_2$ falls from its mid-year maximum to a minimum at New Year at the same time as the $p\text{CO}_2$ in the atmosphere has risen half-way towards its peak in May. It can be argued that active transfer of CO_2 from seawater occurs sooner, from about April as $p\text{CO}_2$ in air is falling to a minimum in October, then beginning to rise as $f\text{CO}_2$ falls to its minimum in mid-winter. Thus, we conclude that the cycle in seawater feeds the cycle in air with a three-month lag. This pattern could easily be shown as six-month periods for each phase, either ascending or descending but offset by about three months. If the $p\text{CO}_2$ values in air [43] have not been corrected for dilution with water vapor then they would be too high by up to 10 ppmv with a greater discrepancy towards the summer minimum giving a much greater overlap with the seawater fugacity driving the increase in $p\text{CO}_2$ in air more strongly in winter. To what extent this process is driven biotically versus abiotically it is difficult to decide, although satellite evidence of chlorophyll content of surface seawater [43] favors the former mechanism.

We have summarized these summer and winter processes in the North Pacific surface layers in Figure 9. Assuming that CO_2 can be transferred to air in winter reaching its maximum value in April despite non-equilibrium process with unfavorable fugacity estimates the hypothesis of an oceanic source for the seasonal oscillation, at least in substantial part, gains credence. These reversible transfers are thermodynamically directed by one phase with strongly varying chemical potentials in seawater interacting with the other phase of air, far less variable in chemical potential, allowing CO_2 a window for transfer from one phase to another. In Figure 8, the stoichiometry of Equation (20) is achieved by taking $(1 + \psi)$ equal to Σ , allowing the dual role of bicarbonate as the source of inorganic carbon for calcite precipitation and as the source for CO_2 for photosynthesis to be achieved.

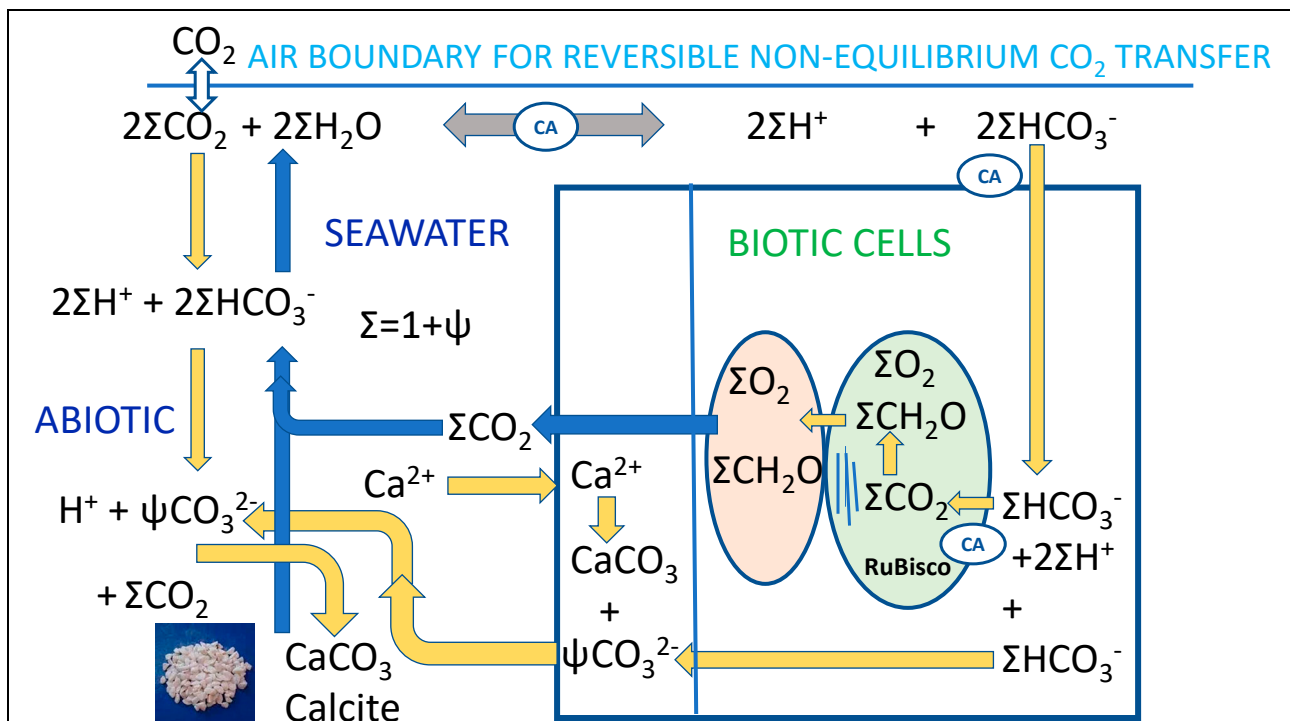


Figure 9. Abiotic and biotic processes for calcite formation and dissolution in surface seawater. Predominant seasonal processes are shown as summer (yellow) and winter (blue), including composite reactions according to Equation (20) involving emission and absorption of CO_2 . Activity by phytoplankton at the boundary layer with air, possibly using carbonic anhydrase (CA) to generate CO_2 or bicarbonate. Abiotic and biotic processes can achieve calcification independently, though responsive to many factors in common.

In this research the Thermal model has had value in showing the effect of temperature variation on the redistribution of DIC between the main species of interest, carbonate, bicarbonate and CO_2 . It has also shown that interconversion between bicarbonate and carbonate and the change in carbonic alkalinity requires accounting for seasonal oscillations in carbonate, decreasing in winter and increasing in summer, a prerequisite for calcite dissolution and precipitation. Such numerical models cannot prove a scientific hypothesis but they do play a metaphysical role in explanation, indicating essential requirements or constraints. Perhaps a major conclusion possible from the complex system shown in Figure 9 is how the ecology of the ocean benefits mutually from a partnership between physicochemical and biological evolution, in which neither operates alone. Completely inorganic processes in seawater may not explain the scale of the seasonal oscillation of $p\text{CO}_2$ in the atmosphere, because the rates of interconversions between the chemical species may be too slow. Figure 9 also indicates how the prolific occurrence of the enzyme carbonic anhydrase in surface seawater can increase the rate of interconversion between bicarbonate and CO_2 in water many orders of magnitude, having also been shown to catalyze the dissolution of calcite in seawater in winter [48]. Extracellular carbonic anhydrase has been considered a key factor in raising CO_2 concentration in seawater at the boundary layer of the ocean [49], so there is precedence for considering higher levels of bicarbonate might elevate CO_2 concentration. The rate of interconversion of bicarbonate and carbonate is inherently fast and does not require catalysis.

5.3. Absence of Similar Data in the Southern Hemisphere

Despite the prevalent opinion of a biological cause for the oscillation, little convincing evidence from measurement of photosynthesis or respiration, either from surface or satellite data in support of the terrestrial cause can be cited, or on the tundra near Point Barrow. Despite the expectation that the large closure of global industry during the COVID-19 pandemic, no clear effect on the progress of the signals from Mauna Loa or Point Barrow was reported. A more precise physico-chemical explanation producing such regular phenomena at multiple sites should be preferred, consistent with Occam's principle.

The smaller magnitude of the oscillation at Cape Grim needs proof for a physical explanation. Despite the Earth receiving more insolation in the southern hemisphere summer being closer to the sun at aphelion, it receives less in the southern hemisphere winter; the range of southern ocean surface temperatures from Ceres satellite data [50] is about 4.7 K versus 7 K in the northern ocean. Isolation at the top of the atmosphere is less variable in the northern hemisphere and of higher average intensity. This is consistent with the range in $p\text{CO}_2$ and hence calcite precipitation being twice as much if one compares data from Barrow with that of Mauna Loa, but the air temperature range at Cape Grim is about the same as near Barrow, although Cape Grim is considerably warmer. Other factors such as the poise of carbonate concentration with respect to saturation (Ω) may be involved to explain the difference between hemispheres. Given that the northern hemisphere ocean basins are significantly warmer but oscillating more strongly in temperature near freezing in polar conditions as at Point Barrow, there may be an inherent inability to concentrate the base level of carbonate in the southern hemisphere. Such repeated freezing and thawing is an effective means of increasing concentration of solutes as the proportion of liquid water declines.

The mixing layer in the Southern Ocean extending to Antarctica is buffeted with higher wind speeds and its surface convection is therefore deeper than in the northern Pacific Ocean [1]. As shown in Figure 3 and Table 2, calcite is more soluble at lower temperatures so accumulation of a higher alkalinity at Point Barrow is possible. It is proposed that the absence of strong seasonal oscillations in $p\text{CO}_2$ at Cape Grim is explained by the relative absence of a seasonal calcite- CO_2 cycle rather than a small disparity between photosynthesis and respiration. Field experimentation is warranted to test the thermal variation hypothesis near Cape Grim, examining the scale of any reversible calcite formation that is predicted to be smaller than at Hilo, Hawaii or Point Barrow, Alaska.

5.4. Weighing the Available Evidence

Predictions from the Thermal model of Figure 2 are consistent with the global field results reported by Takahashi et al. [51] who found that widespread observations of the ocean surface layer show lower alkalinity in summer, particularly in the northern hemisphere as at Point Barrow, as expected if calcite is precipitated. Other measurements reported by Takahashi et al. such as reduced DIC and increased Ω in summer also agree with the Thermal model's prediction. However, their lower calculated pH values in winter are at variance with the predicted result in Figure 5, where seawater pH is more alkaline as anticipated in a solution with more carbonic alkalinity. The flaw exposed in the Thermal model is solved by the interpretation of calcification given in Section 5.3, showing that CO_2 is consumed as carbonate is converted to bicarbonate (Equation (18)) and that seawater and air are several months out of phase with respect to $p\text{CO}_2$ contents.

Assessment of seasonal carbonate cycles in the Southern Ocean differ from those in the northern hemisphere oceans, with less temperature variation. Below the Antarctic circumpolar current the annual mean pH observed with Argo robots is 0.03 units lower and the $f\text{CO}_2$ of seawater higher [7]. Attributions by winter upwelling of DIC and alkalinity may be in part a temperature effect, signaling some dissolution of calcite as discussed in Section 5.2. This novelty regarding thermal effects is despite demonstrated understanding of the physical chemistry of the DIC inorganic reactions involved, published widely in IPCC reports. The key omission is failure to understand how the individual chemical reactions can couple in a concerted manner to achieve this result, as given in Figure 2. Variations in these constants including the Henry coefficient with temperature are likely to be critical information in explaining large scale releases or absorption of CO_2 as ocean currents move between different latitudes. While the proposal regarding purely inorganic calcite precipitation from seawater in summer is novel this will be no surprise to chemical engineers who deal with serious scaling from CaCO_3 precipitation from hard waters, just as observed in kitchen kettles. As Figure 8 shows, this possibility includes significant biological reactions forming CaCO_3 in summer and releasing maximum CO_2 in winter. Calcite may be formed either internally or externally to the cells of marine organisms. A significant scale for the difference between biotic CO_2 assimilation in summer by photosynthesis and its respiratory emission in the colder season lacks quantitative evidence.

The second demonstration emphasized in this article is how dependent inorganic calcite formation is on absolute temperature. The mean temperature of the Earth's surface is close to 288 K in a zone where seasonal oscillation in inorganic calcite is also likely, although regional variation in total alkalinity (A_c) and DIC content (C) can mean that precipitation is still possible across a wider range of temperatures. Although the solubility product for calcite and other forms of CaCO_3 is only moderately responsive to temperature (Table 1), the strong seasonal shifts of the DIC reactions towards increasing thermodynamic potential for $[\text{CO}_2]$ in winter and carbonate in summer for thermodynamic reasons is the main basis of the thermal hypothesis.

The global rates of inorganic precipitation and dissolution of CaCO_3 are not well established. Although biotic calcification is more rapid while sufficient nutrients (P, N, etc.) for growth are available, the relative contribution of the two modes of calcification to geological limestone formation is unclear. However, Burton and Walter [52] demonstrated significant rates of aragonite and calcite precipitation from supersaturated seawater as a function of increasing temperature, with the former predominant above 5 °C, some four times greater at 25 °C at the same saturation. Their data suggests a rate of laboratory precipitation of about 1 mole of CaCO_3 per fortnight per g of crystal seeds, each 3 g shown to exhibit about 1 m² of surface area. About 50 µg of crystal seeds per kg of seawater (i.e., 0.5 µmoles CaCO_3) could be sufficient to explain the absorption of 2 moles of CO_2 in the summer season. Concern [53] that particulate inorganic carbon might decrease with increasing $p\text{CO}_2$ providing negative feedback affecting CO_2 uptake by the ocean is one indication how much this gap in knowledge on rates of calcite precipitation is.

Conversely, a study of dissolution of calcite above the 100% saturation horizon [54] was considered as contrasting with the conservative paradigm of pelagic CaCO_3 at shallow water depths, with 11.1×10^{12} moles C estimated to be dissolved annually in the Atlantic Ocean, an area of 1.065×10^{12} m^2 . Their oscillation of 2 moles per m^2 recycling as an upper limit for the Keeling oscillation is not unreasonable in this context. Gattuso et al. [55] found in association with corals that inorganic calcification of aragonite increased nearly 3-fold when its saturation increased from 98% to 390%, however they failed to consider the effects of oscillating temperature in their study. Buitenhuis et al. [56] estimated global ocean primary production as about 13 moles C per m^2 annually, in which an annual oscillation in both hemispheres of 1–2 moles per m^2 can readily be accommodated.

These properties related to seasonal shifts in equilibria including for the solubility product for calcite has previously been considered in reviews of the seasonal oscillation in the Keeling curve, although Feely et al. [57] observed significant seasonal variations in saturation ratios in surface calcite and aragonite in the northern hemisphere, with a maximum in summer, consistent with some precipitation. Despite $[\text{CO}_2]_{\text{sw}}$ being predicted to be lower in summer from venting to the atmosphere by the large change in the Henry coefficient K_0 , the variations in constants K_1 and K_2 allow $[\text{CO}_3^{2-}]$ to increase in summer. In winter, negative feedback changes in constants K_2 and K_1 ensures that equilibrium $[\text{CO}_2]$ increases sufficiently to support an increasing atmospheric $p\text{CO}_2$. The maximum of DIC measured in seawater at 6 m depth in winter is also consistent with the model of calcite dissolution, although the authors suggested that this observation was a result of the entrainment of high subsurface waters.

This article pays less attention to the scale and important role of biological effects on $p\text{CO}_2$ such as those considered in Fransner et al. [58], studying the effect of nutrients on $p\text{CO}_2$ drawdown in the Gulf of Bothnia in the northern Baltic Sea. However, their observation that primary production needed to reproduce the observed drop in $p\text{CO}_2$ exceeded that they estimated in their study by up to 400%. Rather than adopting their hypothesis-saving suggestion that organic carbon production was underestimated, significant absorption of CO_2 in crystalline CaCO_3 would better explain their observations. This conclusion is consistent with the greater prevalence of land masses above the equator with greater runoff from rainfall into surrounding littoral zones. However, the saturation index for precipitation of calcite is also favored in northern latitudes given the greater prevalence of runoff from rivers of calcium and DIC into the northern ocean basins. The alkalinity and total DIC is known to be greater in northern oceans, particularly nearer the pole. Much greater river runoff also decreases the salt content of northern ocean surface waters, leading to a significant decrease in the solubility product of CaCO_3 , meaning calcite is likely to be formed at a lower concentration of carbonate ions. These factors governing abiotic calcite formation also favor $p\text{CO}_2$ oscillation in the northern hemisphere atmosphere.

5.5. Ambivalence of the Anticorrelation with $^{13}\text{CO}_2$

The lessening ^{13}C -content of atmospheric CO_2 is regarded as evidence for its biological source as in fossil fuels. DIC species in the ocean's surface layer are enriched in this stable isotope, enhanced by the biological pump transferring metabolised carbon to greater depths deposited in the deep ocean. It is claimed that CO_2 in the atmosphere is not derived from the surface layer of the ocean as evidence shows atmospheric CO_2 has a declining heavy isotope content. This observation was interpreted as evidence that increases in the Keeling curve show fossil fuels are the main source of the new CO_2 in air. This may be substantially true for the surface mixed layers of the ocean, but soil carbon is also depleted in ^{13}C -content, given its predominantly biological source with this store of carbon claimed to be twice that in the atmosphere as CO_2 . To the extent that significant increases in release of soil carbon from human activity are possible, this logical proof of the fossil emissions source of CO_2 becomes less convincing.

Furthermore, the anticorrelation of the ^{13}C content of the atmosphere with the $p\text{CO}_2$ of the atmosphere, with the heavy isotope at its lowest value in seawater in the northern

winter is not necessarily proof as has been claimed [59] that the source of elevated CO_2 is mainly terrestrial respiration. Depleted CO_2 from seawater is also possible if its source is from seawater respiration of organic detritus as dissolved organic carbon, fixed the previous summer. Depletion of ^{13}C is also by no means exclusive to biological systems like photosynthesis. Yumol et al. [60] show how CO_2 hydration at the surface can deplete gaseous ^{13}C some -29.7% potentially enriching air with $^{13}\text{CO}_2$ in the summer season. Wanninkhof [61] claimed much lower enrichment from this process. Becker et al. [62] did not interpret their excellent results from over 4 years for transects of 10 bands of longitude in the North Atlantic as indicating abiotic calcite formation in summer and dissolution in winter, their $^{13}\text{CO}_2$ results are consistent with this hypothesis. The three mol CO_2 per m^2 they claimed was exchanged with the atmosphere and surface water is similar to that modelled in this paper. The peak ^{13}C in $[\text{CO}_2]$ in summer and the declining value in the winter season is consistent with the abiotic model presented here. Dissolution and fractionation of the lighter versions of carbonate, and bicarbonate as calcite is dissolved in winter must result in a lower enrichment in the $[\text{CO}_2]$ pool in the surface layer.

The claims by Henzler et al. [63] that CaCO_3 nucleation in supersaturated seawater is likely to be predominantly classical with simple ions or ion pairs a majority is not disputed by our temperature variation hypothesis, given that though carbonate ions must increase in summer at warmer temperature seawater still contains mainly free ions of carbonate, carbonate increasing or declining only some 10% in our modelling. Their thermodynamic data was estimated at 298 K with no temperature variation included in their calculations. Broecker and Peng [64] pointed out the uncertainties in using ^{13}C depletion as a means to calculate CO_2 uptake by the ocean from fossil carbon is problematical, given inaccuracy in the available data set. Tans et al. [65] also question the uncertainty in such calculation. The observation of the diminution of the heavy isotope of carbon in air to fossil fuels is attributed to Quay et al. [66] however this conclusion may need more assessment, given that inorganic carbon in soils can also have a biogenic source.

Despite the ability to model CO_2 transfers successfully in terms of isotopic discrimination, this is by no means proof that these transfers apply if methods are guided by results being consistent with observations. Predictions made by models are far more convincing if made prior to the observations. Nonetheless, researchers are invited to test the hypotheses made in Figures 2 and 9 for consistency with the predicted outcomes.

6. Conclusions

This article advances a novel thermodynamic hypothesis regarding significant physicochemical and abiotic control of atmospheric $p\text{CO}_2$ by surface seawater temperature, rather than solely by kinetic control from terrestrial or aquatic processes. Despite important roles for advection and convection of seawater in short term transport of DIC, venting of CO_2 to the atmosphere or its reabsorption should also be controlled by seasonal variations in chemical potential of DIC species in surface seawater. An earlier report [67] that alkalinity (A_c) within subtropical gyres of the north and south Pacific Ocean remained extremely constant seasonally, allowing seawater fugacity for CO_2 to be calculated directly as a function of temperature is not borne out in more recent studies [7,39,42] and more direct measurements [43] of DIC as bicarbonate and carbonate are needed. The factual nature of the increasing but oscillating Keeling curve is beyond dispute [68] but a better understanding of how it is generated and might be controlled is essential. This article shows that many of the observations made on seawater regarding analyses of DIC and alkalinity [69] that assume biotic processes exclusively can in part be explained by inorganic processes, governed by variations in temperature in seawater. Our study has also shown that the key reactions involving DIC match the seasons regarding their enthalpy changes (Tables 1 and 4) being endothermic (summer) or exothermic (winter), showing that algorithms employed to estimate equilibrium K values [2] are soundly based thermodynamically.

We regard the novel contributions of our modelling study in this article as threefold. First, just as there is a seasonal oscillation in $p\text{CO}_2$ in the global atmosphere, most strongly

in the Northern hemisphere, there must be, assisted thermodynamically, a similar oscillation in inorganic carbon as DIC and CaCO_3 in the surface layer of the ocean, proportional to temperature variation. Calcite formed abiotically does not need to generate net organic carbon production annually, simply adding marginally to that in suspension in summer and diminishing to the same extent in winter. However, biotic processes clearly have greater potential to catalyze net calcification, as a function of available nutrients, solar radiation and other environmental factors. Second, our study provides a more logical framework for calcification processes shown in Equation (20) and Figure 9, better explaining stoichiometrically how bicarbonate, seawater's main carbon constituent, can act reversibly as a source of carbon for CaCO_3 formation, for reversible transfer of CO_2 to the atmosphere and for major biogenic processes. Essential to these processes is the seawater evolution of CO_2 in spring and summer and its consumption in autumn and winter as bicarbonate activity is respectively lowered or increased, conversely with carbonate activity (Equations (18)–(20)). To the extent that calcite is formed in summer, there will be a reduction in DIC alkalinity and a process of acidification according to Equation (2). Third, our study provides a mechanism for attributing most of the seasonal oscillation of $p\text{CO}_2$ in the atmosphere peaking in early spring to the ocean. Research aiming to find terrestrial sources for the oscillation, particularly in the northern tundra, has not been convincing. However, seasonal processes on land can obviously still make some contribution to the oscillation on land, where Keeling first made his unique observations [70], showing a pattern for variable CO_2 content of air where formerly, there was none.

Obviously, predictions from the Thermal hypothesis outlined in Figures 2 and 9, based on variations in temperature in the surface mixing layer, still require rigorous experimental testing in both laboratory and field. There is clearly a role for extension of modelling similar to that shown in this article to plan more directed collection of seasonal datasets for comparisons. Modelling can be explanatory, but cannot alone confirm a hypothesis. Critical mechanistic factors to be examined experimentally include rates of inorganic calcite or aragonite precipitation and dissolution with changes in temperature, transfer rates and thermodynamic control of emission and reabsorption of CO_2 at the seawater-air boundary interface, e.g., [43,45] and the interaction between biotic and abiotic processes, particularly in catalysis of inorganic reactions such as by carbonic anhydrase. Roles for inorganic processes and pseudo-equilibrium control such as that for CO_2 diffusion between seawater layers may be much broader than explaining the seasonal oscillations in the progressive Keeling curve of increasing $p\text{CO}_2$.

We claim too little regard has been paid to the periodic forcing nature of temperature variation globally, even on a daily basis, in predicting evolutionary trends in climate [71]. This neglect is made more acute given the potential resonant effect of such environmental frequencies in phase on fluctuations based on chemical potentials. This paper's main thesis is that short term variations in the $p\text{CO}_2$ in air are largely an inevitable result of changes in temperature, simultaneous with accumulation and breakdown of biomass. If so, CO_2 is thermodynamically and statistically bound to distribute automatically and reversibly between the phases of air and water on the Earth's surface, including on land. This viewpoint is offered for experimental testing and as guidance for possible regulation of CO_2 in the atmosphere and better understanding of how human activities are affecting the global carbon cycle. We call for critical experimental tests of this thermal hypothesis to be conducted as soon as possible.

Supplementary Materials: The following supporting information can be downloaded at: <https://www.mdpi.com/article/10.3390/thermo2040028/s1>, 1. Table S1. Astrocal Thermal showing seasonal variation in $p\text{CO}_2$ correlated inversely with variations in carbonate and calcite solubility shown in Table 3; 2. Table S2. Year 2000 Thermal data values for Point Barrow Alaska in Figures 6 and 7; 3. Figure S1. NCCARF plot of ALOHA Station Data; 4. Table S3. The Thermal Texas Instruments SR52 Program for carbonate chemistry; 5. Table S4. SR52 program to calculate enthalpy, Gibbs energy and entropy; 6. Table S5. Emerson and Hedges Carbonate Chemistry algorithms. Contact ivan.kennedy@sydney.edu.au for further explanation.

Author Contributions: Conceptualization, I.R.K., S.Z.; methodology, I.R.K., R.J.R.; software, I.R.K.; validation, J.W.R., S.Z. and R.J.R.; formal analysis, I.R.K.; investigation, S.Z. and J.W.R.; data curation, I.R.K.; writing—original draft preparation, I.R.K.; writing—review and editing, J.W.R., S.Z. and I.R.K. All authors have read and agreed to the published version of the manuscript.

Funding: This research received no specific external funding, other than general maintenance by employers. This preserves objectivity.

Data Availability Statement: All data generated is included in the text, or in Supplementary Material, using algorithms from Emerson and Hedges [63]. The $\text{CO}_2/\text{HCO}_3^-/\text{CO}_3^{2-}$ calculator used for Figure 3 is an Excel routine (RJR), based on the work of Dickson and Millero [32] and Millero [34] and is available on request. As atmospheric CO_2 varies the Excel routine includes an ongoing fit to the Keeling Curve (Figure 1), allowing variation in temperature, salinity and pH.

Acknowledgments: Our thanks for recent advice in preparing this manuscript go particularly to Susan Agar of Atlas Impacts LLC, USA, Philip Kuchel, Angus Crossan and Robert Caldwell of the University of Sydney and Edward Cocking of Nottingham University. We also acknowledge very useful critique of the first version of this article by three anonymous reviewers and the Chief Editor of this journal, Johan Jacquemin, in achieving a major revision. The causative calcification and decalcification processes shown in Figure 9 were not obvious in the first version available on-line. The senior author dedicates this work to the late Michael Raupach, a research colleague at CSIRO in volatile chemicals research, who suggested at one of our climate science sessions for environmental chemistry students in Canberra that the way to proceed with the central idea in this paper was by modelling testable hypotheses. We also dedicate the paper to the late Lily Pereg who died tragically, a former student who came from Israel as a marine biologist. Her memory inspires this renewed interest in causes of barrier reef formation.

Conflicts of Interest: The authors declare no conflict of interest.

References

1. Harvey, L.D. *Global Warming. The Hard Science*; Prentice Hall: Harlow, UK, 2000.
2. Emerson, S.; Hedges, J. Carbonate Chemistry. In *Chemical Oceanography and Marine Carbon Cycle*; Cambridge University Press: Cambridge, UK, 2008; pp. 101–133.
3. Prentice, I.C.; Farquhar, M.J.R.; Fasham, M.L.; Goulden, M.L.; Heimann, M.; Jarmilla, V.J.; Kheshgi, H.S.; Le Quere, C.; Scholes, R.J.; Wallace, D.W.R. The carbon cycle and atmospheric carbon dioxide. In *Climate Change, Chapter 3 The Scientific Basis, Contribution to the Third Assessment Report of the IPCC*; Cambridge University Press: Cambridge, UK, 2001.
4. Pales, J.C. The concentration of atmospheric carbon dioxide in Hawaii. *J. Geophys. Res.* **1965**, *70*, 6053–6076. [[CrossRef](#)]
5. Keeling, C.D.; Wahlen, M.; van der Plicht, J. Interannual extremes in the rate of rise of atmospheric carbon dioxide since 1980. *Nature* **1995**, *375*, 666–670. [[CrossRef](#)]
6. Foucher, P.Y.; Chédin, A.; Armante, R.; Boone, C.; Crevoisier, C.; Bernath, P. Carbon dioxide atmospheric profiles retrieved from space observation using ACE-FTS solar occultation instrument. *Atmos. Chem. Phys.* **2011**, *11*, 2455–2470. [[CrossRef](#)]
7. Williams, N.L.; Juranek, L.W.; Feely, R.A.; Russell, J.L.; Johnson, K.S.; Hales, B. Assessment of the carbonate chemistry seasonal cycles in the Southern Ocean from persistent observational platforms. *J. Geophys. Res. Oceans* **2018**, *123*, 4833–4852. [[CrossRef](#)]
8. Dore, J.E.R.; Sadler, D.W.; Church, M.J.; Karl, D.M. Physical and biogeochemical modulation of ocean acidification in the central North Pacific. *Proc. Nat. Acad. Sci. USA* **2009**, *106*, 12235–12240. [[CrossRef](#)] [[PubMed](#)]
9. Barker, S.; Ridgwell, A. Ocean acidification. *Nature Educ. Know.* **2012**, *3*, 21.
10. DeVries, T.; Holzer, M.; Primeau, F. Recent increase in oceanic carbon uptake driven by weaker upper ocean overturning. *Nature* **2017**, *542*, 215–218. [[CrossRef](#)]
11. Mackay, D. *Multimedia Environmental Models; The Fugacity Approach*, 2nd ed.; Lewis Publishers: Boca Raton, FL, USA, 2001; p. 166.
12. Dickson, A.G.; Sabine, C.L.; Christian, J.R. *Guide to Best Practices for Ocean CO_2 Measurements*; PICES Special Publication 3, North Pacific Marine Science Organization: Sidney, Canada, 2007.
13. Sander, R. Compilation of Henry's Law constants (Version 4) for water as solvent. *Atmos. Chem. Phys.* **2015**, *15*, 4399–4981. [[CrossRef](#)]
14. Moore, W.J. *Physical Chemistry*, 4th ed.; Prentice-Hall: Hoboken, NJ, USA, 1972.
15. Berner, R.A. Activity coefficients of bicarbonate, carbonate and calcium ions in sea water. *Geochim. Cosmochim. Acta* **1965**, *29*, 947–965. [[CrossRef](#)]
16. Wells, R.C. The solubility of calcite in water in contact with the atmosphere, and its variation with temperature. *J. Wash. Acad. Sci.* **1915**, *5*, 617–622.
17. Mucci, A. The solubility of calcite and aragonite in seawater at various salinities, temperatures, and one atmosphere total pressure. *Amer. J. Sci.* **1985**, *283*, 780–799. [[CrossRef](#)]

18. Plath, D.C.; Johnson, K.S.; Pytkowicz, M. The solubility of calcite—Probably containing magnesium—In Seawater. *Mar. Chem.* **1980**, *10*, 9–29. [[CrossRef](#)]
19. Millero, F.J.; Graham, T.B.; Huang, F.; Bustos-Serrano, H.; Pierrot, D. Dissociation constants of carbonic acid in seawater as a function of salinity and temperature. *Mar. Chem.* **2006**, *100*, 80–94. [[CrossRef](#)]
20. Kane, R.P.; de Paula, E.R. Atmospheric CO₂ changes at Mauna Loa, Hawaii. *J. Atmos. Terres. Phys.* **1996**, *58*, 1673–1681. [[CrossRef](#)]
21. Feely, R.A.; Doney, S.C.; Cooley, S.R. Ocean acidification: Present conditions and future changes in a high-CO₂ world. *Oceanography* **2009**, *22*, 36–47. [[CrossRef](#)]
22. McConnaughey, T.A.; Whelan, J.F. Calcification generates protons for nutrient and bicarbonate uptake. *Ear. Sci. Rev.* **1997**, *42*, 95–117. [[CrossRef](#)]
23. ZarKogiannis, S.D.; Iwasaki, S.; Rae, J.W.B.; Schmidt, M.; Mortyn, P.G.; Kontakiotis, G.; Hertzberg, J.E.; Rikaby, R.E.M. Calcification, dissolution and test properties of modern planktonic foraminifera from the central Atlantic Ocean. *Front. Mar. Sci.* **2022**. [[CrossRef](#)]
24. Raven, J.A.; Johnston, A.M.; Kübler, J.E.; Korb, R.; McInroy, S.G.; Handley, L.L.; Walker, D.I.; Beardall, J.; Clayton, M.N.; Vanderklift, M.; et al. Seaweeds in cold seas: Evolution and carbon acquisition. *Ann. Bot.* **2002**, *90*, 525–536. [[CrossRef](#)]
25. Orr, J.C.; Epitalon, J.M.; Gattuso, J.P. Comparison of ten packages that compute ocean carbonate chemistry. *Biogeosciences* **2015**, *12*, 1483–1510. [[CrossRef](#)]
26. Saruhashi, K. On the equilibrium concentration ratio of carbonic acid substances dissolved in natural water. *Meteor. Geophys.* **1955**, *6*, 38–65. [[CrossRef](#)]
27. Gieskes, J.M. Effect of temperature on the pH of seawater. *Limnol. Oceanog.* **1969**, *14*, 679–685. [[CrossRef](#)]
28. Pytkowicz, R.M. Chemical solution of calcium carbonate in sea water. *Amer. Zool.* **1969**, *9*, 673–679. [[CrossRef](#)]
29. Mehrbach, C.; Culberon, C.H.; Hawley, J.E.; Pytkowicz, R.M. Measurement of the apparent dissociation constants of carbonic acid in seawater at atmospheric pressure. *Limnol. Oceanog.* **1973**, *18*, 897–907. [[CrossRef](#)]
30. Bailey, N.; Papakyriakou, T.N.; Bartels, C.; Wang, F. Henry's Law constant for CO₂ in aqueous sodium chloride solutions at 1 atm and sub-zero (Celsius) temperatures. *Mar. Chem.* **2018**, *2017*, 26–32. [[CrossRef](#)]
31. Ingle, S.E. Solubility of calcite in the ocean. *Mar. Chem.* **1975**, *3*, 301–319. [[CrossRef](#)]
32. Dickson, A.G.; Millero, F.J. A comparison of the equilibrium constants for dissociation of carbonic acid in seawater media. *Deep Sea Res.* **1987**, *34*, 1733–1743. [[CrossRef](#)]
33. Dickson, A.G.; Goyet, C. *Handbook of Methods for the Analysis of Various Parameters of the Carbon Dioxide System in Sea Water. Version 2*; ORNL/CDIAC-74; Oak Ridge National Lab: Oak Ridge, TN, USA, 1994.
34. Millero, F.J. Thermodynamics of the carbon dioxide system in the oceans. *Geoch. Cosmo. Acta* **1995**, *59*, 661–677. [[CrossRef](#)]
35. Millero, F.; Huang, F.; Graham, T.; Pierrot, D. The dissociation of carbonic acid in NaCl solutions as a function of concentration and temperature. *Geochim. Cosmochim. Acta* **2007**, *71*, 46–55. [[CrossRef](#)]
36. Kanwisher, J. pCO₂ in sea water and its effect on the movement of CO₂ in Nature. *Tellus* **1960**, *12*, 209–215. [[CrossRef](#)]
37. Morin, S.; Marion, G.M.; von Glasow, R.; Voisin, D.; Bouchez, J.; Savarino, J. Precipitation of salts in freezing seawater and ozone depletion events: A status report. *Atmos. Chem. Phys.* **2009**, *8*, 9035–9060. [[CrossRef](#)]
38. Hu, Y.B.; Wolf-Gladrow, D.A.; Dieckmann, G.S.; Völker, C.; Nehrke, G. A laboratory study of ikaite (CaCO₃·6H₂O) precipitation as a function of pH, salinity, temperature and phosphate concentration. *Mar. Chem.* **2014**, *162*, 10–18. [[CrossRef](#)]
39. Takahashi, T.; Olafsson, J. Seasonal variation of CO₂ and nutrients in the high-latitude surface oceans: A comparative study. *Glob. Biogeochem. Cycl.* **1993**, *7*, 843–878. [[CrossRef](#)]
40. Zeebe, R.E.; Westbroek, P. A simple model for the CaCO₃ saturation state of the ocean: The “Strangelove”, the “Neritan” and the “Cretan” ocean. *Geochim. Geophys. Geosys.* **2003**, *4*, 1–26. [[CrossRef](#)]
41. Watson, S.A.; Fabricius, K.E.; Munday, P.L. Quantifying pCO₂ in biological ocean acidification experiments: A comparison of four methods. *PLoS ONE* **2017**, *12*, 1–16. [[CrossRef](#)]
42. Quay, P.; Stutsman, J. Surface layer carbon budget for the subtropical N. Pacific: δ¹³C constraints at station ALOHA. *Deep. Sea Res.* **2003**, *50*, 1045–1061. [[CrossRef](#)]
43. Chen, S.; Sutton, A.J.; Hu, C. Quantifying the atmospheric CO₂ forcing effect on surface ocean pCO₂ in the North Pacific subtropical gyre in the past two decades. *Front. Mar. Sci.* **2021**, *8*, 636861.
44. Morowitz, H.J. *Energy Flow in Biology. Biological Organization as a Problem in Thermal Physics*; Ox Bow Press: Woodbridge, VA, USA, 1968.
45. Sutton, A.J.; Sabine, C.L.; Maenner-Jones, S.; Lawrence-Slavas, N.; Meinig, C.; Feely, R.A.; Mathis, J.T.; Musielewicz, S.; Bott, R.; McLain, P.D.; et al. A high-frequency atmospheric and seawater pCO₂ data set from 14 open-ocean sites using a moored autonomous system. *Earth Syst. Sci. Data* **2014**, *6*, 353–366. [[CrossRef](#)]
46. Smith, S.V. *Parsing the Oceanic Calcium Carbonate Cycle: A Net Atmospheric Carbon Dioxide Source, or a Sink*; L&O e-Books; Anderson, M.R., Ed.; Association Sciences Limnology and Oceanography (ASLO): Waco, TX, USA, 2013. [[CrossRef](#)]
47. Chen-Tung, A.; Pytkowicz, R.M. On the total CO₂-titration alkalinity-oxygen system in the Pacific Ocean. *Nature* **1979**, *281*, 362–365. [[CrossRef](#)]
48. Subhas, A.V.; Adkins, J.F.; Rollins, N.E.; Naviaux, J.; Erez, J.; Berelson, W.M. Catalysis and chemical mechanisms of calcite dissolution in seawater. *Proc. Natl. Acad. Sci. USA* **2017**, *114*, 8175–8180. [[CrossRef](#)]
49. Mustafa, N.I.H.; Latif, M.T.; Wurl, O. The role of extracellular carbonic anhydrase in biogeochemical cycling: Recent advances and climate change responses. *Int. J. Mol. Sci.* **2021**, *22*, 7413. [[CrossRef](#)]

50. Loeb, N.G.; Manalo-Smith, N.; Su, W.; Shnkar, M.; Thomas, S. CERES Top-of Atmosphere Earth radiation budget climate data record: Accounting for in-orbit changes in instrument calibration. *Remote Sens.* **2016**, *8*, 182–196. [CrossRef]
51. Takahashi, T.; Sutherland, S.C.; Chipman, D.W.; Goddard, J.G.; Cheng, H.; Newberger, T.; Sweeney, C.; Munro, D.R. Climatological distributions of pH, $p\text{CO}_2$, total CO_2 , alkalinity, and CaCO_3 saturation in the global surface ocean, and temporal changes at selected locations. *Mar. Chem.* **2014**, *164*, 95–125. [CrossRef]
52. Burton, E.A.; Walter, L.M. Relative precipitation rates of aragonite and Mg calcite from seawater: Temperature or carbonate control? *Geology* **1987**, *15*, 111–114. [CrossRef]
53. Zondervan, I.; Zeebe, R.E.; Rost, B.; Riebesell, U. Decreasing marine biogenic calcification: A negative feedback on rising; Atmospheric $p\text{CO}_2$. *Glob. Biogeochem. Cyc.* **2001**, *15*, 507–516. [CrossRef]
54. Chung, S.N.; Lee, K.; Feely, R.A.; Sabine, C.L.; Millero, F.J.; Wanninkhof, R.; Bullister, J.L.; Key, R.M.; Peng, T.H. Calcium carbonate budget in the Atlantic Ocean based on water column inorganic carbon chemistry. *Glob. Biogeochem. Cyc.* **2003**, *17*, 1093. [CrossRef]
55. Gattuso, J.; Frankignoulle, M.; Bourge, I.; Romaine, S.; Buddemeier, R.W. Effect of calcium carbonate saturation of seawater on coral calcification. *Glob. Planet Change* **1998**, *18*, 37–46. [CrossRef]
56. Buitenhuis, E.T.; Hashioka, T.; Le Quéré, C. Combined constraints on global ocean primary production using observations and models. *Amer. Geophys. Union* **2013**, *27*, 847–858. [CrossRef]
57. Feely, R.A.; Byrne, P.H.; Archer, J.G.; Betzer, G.; Chen, T.A.; Gendron, J.F. Land Winter-summer variations in calcite and aragonite saturation in the northeast Pacific. *Mar. Chem.* **1988**, *25*, 227–241. [CrossRef]
58. Fransner, F.; Gustafsson, E.; Tedesco, L.; Vichi, M.; Hordoir, R.; Roquet, F.; Spilling, K.; Kuznetsov, I.; Eilola, K.; Mörth, C.-M.; et al. Non-Redfieldian dynamics explain seasonal $p\text{CO}_2$ drawdown in the gulf of Bothnia. *J. Geophys. Res. Ocean* **2017**, *123*, 166–168. [CrossRef]
59. Earth System Research Laboratories. The Data: What ^{13}C tells us. The Global View. Global Monitoring Laboratory; 2017. Available online: <https://gml.noaa.gov/ccgg/isotopes/c13tellsus.html> (accessed on 13 July 2022).
60. Yumol, L.M.; Uchikawa, T.; Zeebe, R.E. Kinetic isotope effects during CO_2 hydration: Experimental results for carbon and oxygen fractionation. *Geochim. Cosmochim. Acta* **2020**, *279*, 189–203. [CrossRef]
61. Wanninkhof, R. Kinetic fractionation of the carbon isotopes ^{13}C and ^{12}C during transfer of CO_2 from air to seawater. *Tellus B Chem. Phys. Meteor.* **1985**, *37*, 128–135. [CrossRef]
62. Becker, M.; Steinhoff, T.; Kortzinger, A. A detailed view of the seasonality of stable carbon isotopes across the North Atlantic. *Adv. Earth Space Sci.* **2018**, *32*, 1406–1419. [CrossRef]
63. Henzler, K.; Fetisov, E.O.; Galib, M.; Baer, M.D.; Legg, B.A.; Borca, C.; Xto, J.C.; Pin, S.; Fulton, J.L.; Schenter, G.K.; et al. Supersaturated calcium carbonate solutions are classical. *Sci. Adv.* **2018**, *4*, eaa06283. [CrossRef] [PubMed]
64. Broecker, W.S.; Peng, T.H. Evaluation of the ^{13}C constraint on the uptake of fossil fuel CO_2 by the ocean. *Glo. Biogeochem. Cyc.* **1993**, *7*, 619–626. [CrossRef]
65. Tans, P.P.; Berry, J.A.; Keeling, R.F. Oceanic $^{13}\text{C}/^{12}\text{C}$ observations: A new window on ocean CO_2 uptake. *Glob. Biogeochem. Cyc.* **1993**, *7*, 353–368. [CrossRef]
66. Quay, P.D.; Tilbrook, B.; Wong, C.S. Oceanic uptake of fossil fuel CO_2 : Carbon-13 evidence. *Science* **1992**, *256*, 74–79. [CrossRef] [PubMed]
67. Weiss, R.F.; Jahnke, R.R.; Keeling, C.D. Seasonal effects of temperature and salinity on the partial pressure of CO_2 in seawater. *Nature* **1982**, *300*, 511–513. [CrossRef]
68. Ciais, P.; Sabine, C.; Balu, G.; Bopp, L.; Brovkin, V.; Canadell, J.; Chahabra, A.; Defries, R.; Galloway, J.; Heimann, M.; et al. Carbon and other biogeochemical cycles. In *Climate Change; The Physical Science Basis Contribution of Working Group I to Fifth Assessment Report of the IPCC*; Stocker, T.F., Qin, D., Plattner, G.-K., Tignor, M., Allen, S.K., Boschung, J., Nauels, A., Xia, Y., Bex, V., Midgley, P.M., Eds.; Cambridge University Press: Cambridge, UK, 2013.
69. Middelberg, J.J.; Soetaert, K.; Hagens, M. Ocean alkalinity, buffering and biogeochemical processes. *Rev. Geophys.* **2020**, *58*, e2019RG000681. [CrossRef]
70. Keeling, C.D. Is carbon dioxide from fossil fuel changing man's environment? *Proc. Amer. Philosoph. Soc.* **1970**, *114*, 10–17.
71. Watterson, I.G. The diurnal cycle of surface air temperature in simulated present and doubled CO_2 climates. *Clim. Dynam.* **1997**, *13*, 533–545. [CrossRef]